JCI insight

Airway surveillance and lung viral control by memory T cells induced by COVID-19 mRNA vaccine

Brock Kingstad-Bakke, … , Yoshihiro Kawaoka, M. Suresh

JCI Insight. 2023. https://doi.org/10.1172/jci.insight.172510.

Research In-Press Preview COVID-19 Immunology

Graphical abstract

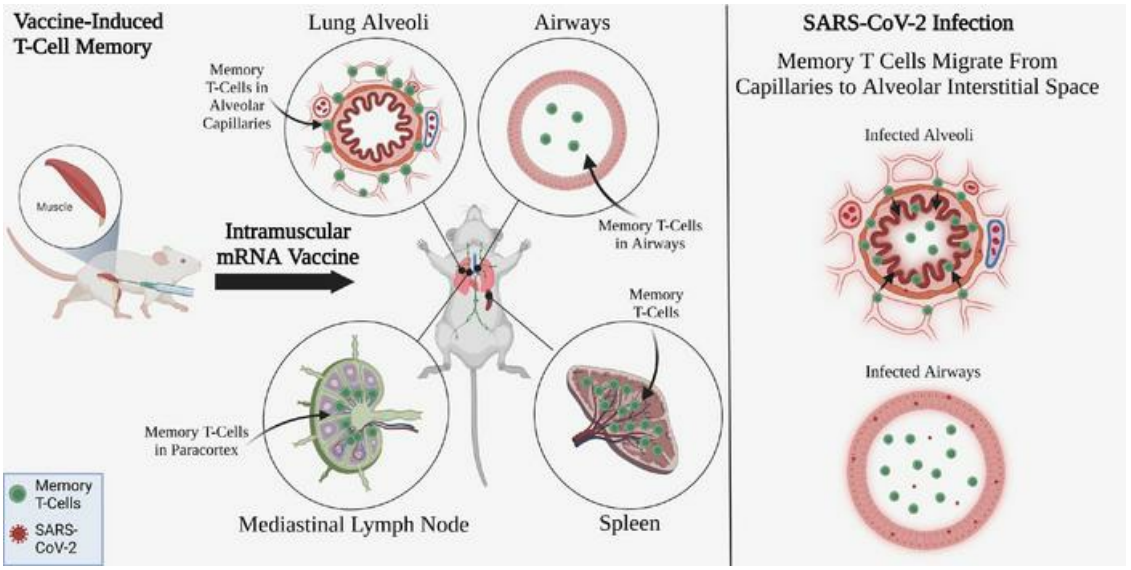

Find the latest version:

https://jci.me/172510/pdf

Airway Surveillance and Lung Viral Control by Memory T Cells Induced by COVID-19 mRNA Vaccine

Brock Kingstad-Bakke[1]**, Thomas Cleven[1]**, Hailey Bussan[1], Boyd L. Yount Jr.[2], Ryuta Uraki[3,4], Kiyoko Iwatsuki-Horimoto[3], Michiko Koga[5,6], Shinya Yamamoto[3,6], Hiroshi Yotsuyanagi[5,6], Hongtae Park[1], Jay Mishra[7], Sathish Kumar[7], Ralph S. Baric[2], Peter Halfmann[1], Yoshihiro Kawaoka[1,3,4,8], and M. Suresh[1]*

[1]Department of Pathobiological Sciences, University of Wisconsin-Madison, Madison, WI 53706, USA

[2]Department of Microbiology and Immunology, University of North Carolina-Chapel Hill, Chapel Hill, NC 27599, USA.

[3]Division of Virology, Institute of Medical Science, University of Tokyo, Tokyo, Japan.

[4]The Research Center for Global Viral Diseases, National Center for Global Health and Medicine Research Institute, Tokyo, Japan.

[5]Department of Infectious Diseases and Applied Immunology, IMSUT Hospital of The Institute of Medical Science, University of Tokyo, Tokyo, Japan.

[6]Division of Infectious Diseases, Advanced Clinical Research Center, Institute of Medical Science, University of Tokyo, Tokyo, Japan.

[7]Department of Comparative Biosciences, University of Wisconsin-Madison, Madison, WI 53706, USA

[8]The University of Tokyo, Pandemic Preparedness, Infection and Advanced Research Center (UTOPIA), Tokyo, Japan

*Lead Contact: sureshm@vetmed.wisc.edu 608-265-9791

** Contributed equally to this work.

The authors have declared that no conflict of interest exists.

ABSTRACT

Although SARS-CoV-2 evolution seeds a continuous stream of antibody-evasive viral variants, COVID-19 mRNA vaccines provide robust protection against severe disease and hospitalization. Here, we asked whether mRNA vaccine-induced memory T cells limits lung SARS-CoV-2 replication and severe disease. We show that mice and humans receiving booster BioNTech® mRNA vaccine developed potent CD8 T-cell responses and show similar kinetics of expansion and contraction of granzyme B/perforin-expressing effector CD8 T cells. Both monovalent and bivalent mRNA vaccines elicited strong expansion of a heterogeneous pool of terminal effectors and memory precursor effector CD8 T cells in spleen, inguinal and mediastinal lymph nodes, pulmonary vasculature, and most surprisingly in the airways, suggestive of systemic and regional surveillance. Further, we document that: (1) CD8 T-cell memory persists in multiple tissues for >200 days; (2) following challenge with pathogenic SARS-CoV-2, circulating memory CD8 T cells rapidly extravasate to the lungs and promote expeditious viral clearance, by mechanisms that require CD4 T cell help; (3) adoptively transferred splenic memory CD8 T cells traffic to the airways, and promote lung SARS-CoV-2 clearance. These findings provide new insights into the critical role of memory T cells in preventing severe lung disease following breakthrough infections with antibody-evasive SARS-CoV-2 variants.

INTRODUCTION

The rapid development of efficacious mRNA vaccines to combat the SARS-CoV-2 pandemic is one of the greatest medical and scientific achievements of the 21st century. While nucleic acid-based vaccines have been widely known and tested since the mid 1990s, no commercially available DNA or RNA vaccines existed for human use before the advent of lipid nanoparticle Moderna® and Pfizer-BioNTech® mRNA vaccines expressing the SARS-CoV-2 spike gene. To date billions of doses of the COVID-19 mRNA vaccines have been given globally, and numerous studies have demonstrated their effectiveness in reducing severe disease outcomes and death (1-4).

Unlike many inactivated and subunit-based vaccines, mRNA vaccination expresses antigen within cells leading to robust T cell responses, particularly for CD8 T cells, which serve to recognize antigen presented from an intracellular origin. The ability to elicit a potent T cell response may be a major advantage for combating continuous emergence of global variants, because epitopes recognized by CD4 and CD8 T cells and not antibodies are strongly conserved across variants (5). While many studies have documented that CD4 and CD8 T cells elicited by mRNA vaccines strongly correlated with more positive outcomes following infection with SARS-CoV-2, and that these T cell responses are long lived (6-13), incisive studies to determine the protective mechanisms, tissue distribution of memory T cells, or the kinetics of the T cell response at an organ-by-organ level are not possible in humans. Therefore, we developed a non-transgenic mouse model to study the defining characteristics of CD8 T cell responses induced by mRNA vaccinations, and the protective mechanisms underlying the

protection against SARS-CoV-2 in the lungs. We show that the CD8 T cell responses of humans and mice to booster COVID-19 mRNA vaccine are largely similar in the peripheral blood, and provide unequivocal evidence of respiratory (airways, lung vasculature, and mediastinal lymph nodes) and systemic immunosurveillance by memory CD8 T cells that effectively reduce SARS-CoV-2 burden in lungs, by CD4 T cell dependent mechanisms. These findings have provided new insights into the character and anatomy of the T cell response to COVID-19 mRNA vaccine and the CD8 T cell-dependent protective mechanisms against SARS-CoV-2 control in lungs. New insights from this study have significant implications in understanding how COVID-19 mRNA vaccines reduce disease severity and hospitalizations following breakthrough infections, and underscore the prominent role of memory T cells in protection against rapidly evolving antibody-evasive viral variants.

RESULTS

Parenteral COVID-19 mRNA Vaccination Elicits Potent Systemic and Pulmonary Effector CD8 T-Cell Responses in Mice

Previous pre-clinical studies with COVID-19 mRNA vaccines in mice have used doses ranging from 5ug to 20ug (14-17). Our pilot immunogenicity studies with the BioNTech® COVID-19 mRNA vaccine in mice showed that doses of 2.5, 5.0 and 10ug mRNA elicited comparable frequencies of antigen-specific CD8 T cells in spleen, but responses to the 10ug dose showed low variability (**Fig. S1**). Hence, we chose to use 10ug dose for all our experiments described in this manuscript. To determine the magnitude and tissue distribution of the antigen-specific effector CD8 T cell responses elicited by the human BioNTech® COVID-19 mRNA vaccine, we vaccinated cohorts of C57BL/6 mice twice (3 weeks apart) by the intramuscular (IM) route. At days 5 and 8 after the second dose of the vaccine, we analyzed the immunodominant K^b-restricted CD8 T-cell response to S525-532 (S525) epitope (18) in the respiratory tract (airways [broncoalveolar lavage; BAL], lungs and lung-draining mediastinal lymph nodes [mLN]), spleen, and the vaccine-draining lymph node (inguinal lymph node [iLN]). At Day 5 and Day 8, mRNA vaccination elicited remarkably high frequencies of spike-specific CD8 T cells in all tissues measured (**Fig. 1A**). Frequencies and numbers of S525-specific CD8 T cells at Day 5 were slightly higher or similar to those at Day 8, and the percentages of proliferating $Ki67^{+ve}$ S525-specific CD8 T cells dropped substantially between days 5 and 8 (**Fig. 1B**). Based on these data, we inferred that the peak of the response likely occurred in most tissues at D5 after booster vaccination. Most notably, intramuscular immunization elicited unexpectedly high frequencies and numbers of CD8 T cells in respiratory tract-associated tissues (airways, lungs and mLN); frequencies of S525-specific CD8 T cells at D5 and D8 ranged from 12-60% in BAL,

13-52% in lung, and 3-8% in mLN (**Fig 1A**). By performing vascular staining, we assessed whether vaccine-elicited CD8 T cells resided in the lung vasculature or parenchyma. We found that S525-specific CD8 T cells in BAL were completely excluded from vascular staining, and the majority of S525-specific CD8 T cells in the lungs were confined to the pulmonary vasculature (**Fig. 1C**). These findings suggested that mRNA vaccines elicited a strong systemic CD8 T cell response in the spleen, draining LN and non-draining lymph nodes. Additionally, these data suggested that mRNA vaccine elicited high levels of effector CD8 T cells in airways, pulmonary vasculature, and mediastinal lymph nodes, suggestive of regional respiratory surveillance.

Next, we examined the heterogeneity of effector CD8 T cells in various tissues, in terms of their differentiation status based on the expression of the IL-7 receptor (CD127) and the senescence marker KLRG1 i.e., memory precursor effector cells (MPECs; $CD127^{HI}KLRG1^{LO}$) and short-lived effector cells (SLECs; $CD127^{LO}KLRG1^{HI}$) (**Fig. 1D**). At day 5, the percentages of MPECs in lymphoid tissues spleen and LNs were in the range of 15-25%, and these percentages dropped to 5-15% by day 8. The drop in percentages of MPECs in lymphoid tissues was linked to a proportional increase in the percentages of SLECs between days 5 and 8 after vaccination; SLEC accumulation was more pronounced (5-fold increase) in the spleen and BAL between days 5 and 8, which is suggestive of preferential trafficking into and/or accumulation of SLECs in lung airways. It is noteworthy that at day 8 after vaccination, there was a stepwise increase in the MPEC frequencies between spleen, mLNs and iLNs, and a reciprocal and proportional reduction in the frequencies of SLECs in respective tissues. Thus, the vaccine draining LN

(iLN) appeared to support MPEC accumulation more strongly, than spleen and the non-draining lymph node (mLN).

To gain further insight into the differentiation of effectors and memory precursor effectors following mRNA vaccination, we analyzed the co-expression of the effector molecule granzyme B, and the pro-survival transcription factor TCF-1, which is intimately linked to the development of memory T cells (19). First, it should be noted that the COVID-19 mRNA vaccine stimulated in all tissues, robust numbers of bonafide effector CD8 T cells that expressed high levels of granzyme B (**Fig. 2A**). Second, our analysis resolved two distinct subsets of effector T cells that expressed markedly different levels of granzyme B and TCF-1: Granzyme $B^{HI}TCF\text{-}1^{LO}$ (Effector Cells; ECs) and Granzyme $B^{LO}TCF\text{-}1^{HI}$ (Memory Precursor Effectors; MPs) (**Fig. 2A**). Both at day 5 and 8 after vaccination, there was a graded increase in the percentages of MPs in lungs, spleen, mLN and iLN (**Fig. 2A**); reciprocally there was a graded decrease in the percentages of ECs in lungs, spleen, mLN and iLN. We validated flow cytometric quantification of TCF-1 in CD8 T cells by western blot, which showed the expected downregulation of TCF-1 in effector CD8 T cells from spleen of vaccinated mice, as compared to CD8 T cells in spleen of unvaccinated mice (**Fig S2**). The percentages of ECs among S525-specific CD8 T cells were higher in lung vasculature and spleen and the percentages of MPs were highest, especially in the iLNs. Interestingly, like spleen, BAL CD8 T cells contained a mixture of ECs and MPs, but there was a conspicuous enrichment for ECs with very few MPs in the lung vasculature. These data suggests that lung vasculature might preferentially harbor ECs, and accumulation of S525-specific CD8 T cells, especially the MPs in the airways might occur by mechanisms independent of cell trafficking from lung vasculature. As another metric for the differentiation

status of effector CD8 T cells, we quantified the expression of the chemokine receptors, CXCR3 and CX3CR1 (**Fig. 2B**); elevated CX3CR1 expression has been associated with terminal differentiation of CD8 T cells (20, 21). Strikingly, 50-80% of S525-specific CD8 T cells in all tissues, expressed CXCR3. CXCR3 expression in lungs could not be assessed rigorously because enzymatic digestion of the lung tissue led to selective loss of cell surface CXCR3 on the isolated CD8 T cells. However, lungs contained higher percentages of $CX3CR1^{+ve}$ CD8 T cells than in other tissues (**Fig. 2c**). The percentages of $CXCR3^{+}CX3CR1^{-}$ cells in iLNs were higher than in spleen and mLNs (**Fig. 2B**). Taken together, S525-specific effector CD8 T cells in the lung vasculature were enriched for granzyme^{HI}TCF-1^{LO}CD127^{LO} cells, and iLNs contained greater percentages of granzyme B^{LO}TCF-1^{HI}CXCR3^{HI}CD127^{Hi} MP-like effector cells. Furthermore, the composition and differentiation status of effector CD8 T cells in airways mirrored splenic CD8 T cells but not those in the pulmonary vasculature. In sum, the heterogeneous population of antigen-specific CD8 T cells elicited by the mRNA vaccine consisted of bonafide effectors and memory precursors and the relative proportions of these subsets were regulated in a tissue-specific manner. The phenotype and differentiation trajectory of effector CD8 T cells was not significantly affected by the vaccine dose, at least in the spleen (**Fig. S1B**).

It has become increasingly clear that the mutations accrued in the spike protein of the Omicron variant of SARS-CoV-2 have facilitated effective viral evasion of antibodies elicited by the first-generation mRNA vaccines (22-25). Therefore, an updated bivalent mRNA vaccine (containing mRNA encoding the original and the Omicron spike protein) has been used for several months, as a booster vaccine. *In silico* analyses show that unlike B cell epitopes, T cell epitopes in the

Omicron variant spike protein might be conserved across SARS-CoV-2 variants (5). Here, we compared the immunodominant CD8 T cell responses to the original and the new bivalent vaccines. The magnitude, tissue distribution, and differentiation trajectory of effector CD8 T cells elicited by the bivalent vaccine was comparable to those induced by the original mRNA vaccine (**Fig. S3A-C**). Further, S525-specific effector CD8 T cells elicited by the monovalent and bivalent vaccines were functional and displayed a T_C1 polarization (**Fig. S3D**); upon ex vivo peptide stimulation, lung and splenic S525-specific CD8 T cells elicited by both monovalent and bivalent vaccines expressed CD40L and/or IFNγ.

Parenteral mRNA Vaccination Elicits Memory CD8 T Cells in the Respiratory Tract and Lymphoid Tissues

At 96 days after booster mRNA vaccination, we found readily detectable numbers of memory CD8 T cells in the lymphoid tissues spleen, mLNs, and iLNs (**Fig. 3A**). Surprisingly however, we also found high frequencies of memory CD8 T cells localized to the airways and lungs, but memory CD8 T cells in the lungs were largely restricted to the pulmonary vasculature (**Fig. S4A, S4B**). Phenotypically, lymphoid tissues contained largely $CD127^{HI}KLRG1^{LO}$ central memory CD8 T cells (**Fig. 3B** and **3C**). By contrast, airway memory CD8 T cells were largely of the $CD127^{LO}CD27^{LO}CD62L^{LO}KLRG1^{LO}$ effector memory phenotype. Interestingly, airways and lung vasculature were enriched (>60%) for $CD27^{LO}CD62L^{LO}$ memory CD8 T cells, as compared to spleen and lymph nodes. The chemokine receptor CXCR3 plays an important role in T cell migration to inflamed tissues expressing ligands CXCL9/10 (26) and also serves as an indicator of Tc1/Th1 effector differentiation (27). Majority of memory CD8 T cells at D96 expressed high levels of CXCR3, and lack of CXCR3 on lung memory CD8 T cells is likely an

artifact of enzymatic digestion. Like CXCR3, CX3CR1 promotes trafficking of CD8 T cells to inflamed and infected tissues via interactions with its ligand CX3CL1 expressed on endothelial cells. A greater percentage (>50%) of memory CD8 T cells in spleen and lungs expressed elevated levels of CX3CR1, as compared to those in lymph nodes and airways, and notably, spleen contained a distinct subset of $CXCR3^{LO}CX3CR1^{HI}$ memory CD8 T cells (**Fig. 3D**). Thus, a substantive fraction of memory CD8 T cells in circulation or in various tissues express CXCR3 and/or CX3CR1, and hence are poised to rapidly traffic into infected tissues such as lungs, upon infection.

Since we detected robust maintenance of memory CD8 T cells in airways and lung-draining lymph node (mLN), it was of interest to assess whether immunological milieu in these tissues led to mucosal imprinting and expression of tissue-residency markers such as CD103 and CD69. While mRNA vaccines are formulated for and only approved for parenteral use, to serve as a positive control for mucosal imprinting, cohorts of mice were vaccinated with the same mRNA vaccine by the intranasal (IN) route. At 96 days after IM vaccination, except for a very small fraction of the airway memory CD8 T cells, memory CD8 T cells in lungs, spleen or mLNs of IM vaccinated animals did not express CD103 and CD69 (**Fig. S4C**). In comparison, a substantive fraction of lung memory CD8 T cells in the IN vaccinated mice were found in the extravascular lung interstitium, and a fraction of memory CD8 T cells in BAL, lungs, and mLNs of IN vaccinated mice expressed CD103 and CD69 (**Fig. S4C).** Thus, despite trafficking to airways and lung-draining lymph nodes, memory CD8 T cells elicited by intramuscular mRNA vaccination failed to express CD103/CD69 and differentiate into classical tissue-resident memory CD8 T cells.

Notably, granzyme B-expressing effector-like memory CD8 T cells were found in all locations, but the frequencies of such effector-like memory CD8 T cells were conspicuously lower in the airways and mediastinal lymph nodes (**Fig. 3E**). Interestingly however, despite sharing the cell surface phenotype of effector memory cells ($CD62L^{Lo}$), memory CD8 T cells in lung vasculature but not in airways were enriched (60%) for granzyme B expression (**Fig. 3E**). Memory CD8 T cells expressing higher levels of TCF-1 were found in greater frequencies in the lymph nodes, which is consistent with their $CD62L^{HI}CD127^{HI}CD27^{HI}$ central memory phenotype. Expression of T-bet did not differ significantly between tissues, but EOMES expression was higher in lungs and lymph nodes (**Fig. 3F**). In summary, the COVID-19 mRNA vaccine elicited central and granzyme B-expressing effector memory CD8 T cells, which were distributed both systemically (spleen) and locally (draining and non-draining lymph nodes), and in the pulmonary vasculature. Additionally, it is noteworthy that mRNA vaccine programmed a phenotypically, functionally, and transcriptionally distinct cohort of memory CD8 T cells in the lung vasculature.

Next, we determined whether the kinetics of the CD8 T cell response differed in a tissue-specific fashion. After reaching peak levels on day 5 or 8 after booster vaccination, S-specific CD8 T cells contracted in all tissues; as compared to day 5 levels, ~60, 90, and 76% of S-specific CD8 T cells were lost in BAL, spleen, and mLNs respectively. While there were readily detectable levels of memory CD8 T cells in airways, we did not detect any extravasation of vascular memory CD8 T cells into the pulmonary interstitium over time (**Fig. S4A, 5B**). Effector-to-memory transition was associated with enrichment for $CD62L^{+ve}CD127^{+ve}KLRG1^{-ve}$ memory

CD8 T cells in all tissues, but more prominently in spleen and lymph nodes (**Fig. S4D-F**). Expression of CXCR3 and CX3CR1 did not change over time substantially (**Fig. S4G, S2H**).

Kinetics of mRNA-Spike-Specific CD8 T Cells in Peripheral Blood of Mice and Humans

In most human studies, vaccine T cell responses were measured in the peripheral blood. Here, we performed longitudinal analysis of CD8 T cell responses in the circulation of mRNA vaccinated mice and humans and asked whether: (1) murine and human CD8 T cell responses to the COVID-10 mRNA booster vaccine are similar; (2) the magnitude of CD8 T cell response in blood reflect levels in lymphoid tissues and respiratory tract; (3) the peak CD8 T cell levels in blood forecasts the durability and magnitude of CD8 T cell memory. In mice, at the peak of the response (D8) the frequency of S525+ specific CD8 T cells ranged from ~20-50% (**Fig. 4A**), which was similar to frequencies detected in the spleens of vaccinated mice at this time (**Fig. 1A**). These S525+ cells decreased in frequency to ~5% of total CD8s by day 99. The average contraction of CD8 T cells between days 8 and 99 was 10-fold, from ~30% to 3% on average. The magnitude of the peak response correlated with the frequency of CD8 T cells at memory i.e., mice with the highest frequency of S525 specific CD8 T cells at D8 had the highest frequencies at D99. Overtime, the frequencies of cells expressing both CXCR3 and CX3CR1 diminished but there was an enrichment for $CXCR3^{LO}CX3CR1^{HI}$ cells in the circulation (**Fig. 4B**). While low levels of $KLRG1^{HI}$ cells persisted over time, $KLRG1^{HI}CXCR3^{HI}CX3CR1^{HI}$ rapidly contracted after the peak of the response, indicating that these highly differentiated cells might lose expression of one or more of these markers, or that they fail to survive. Overall, S525-specific CD8+ T cells detected in PBMCs in mice displayed similar phenotypes to those in spleen, being $CXCR3^{HI}$, $CX3CR1^{HI}$, $CD69^{LO}$, $CD103^{LO}$, and relatively steady levels of KLRG1,

and levels of CD127 increasing over time, with the peak of PD-1 expression coinciding with recent antigenic exposure (**Fig. 4C**). However, the kinetics of Ki-67 expression in circulating mouse S525-specific CD8 T cells resembled CD8 T cells in the lung vasculature during the peak of the response (**Fig. 1B, S5**), when nearly all cells were in a proliferative state at D5 but proliferation dropped precipitously by D8.

To assess the kinetics of the human CD8 T cell response to booster vaccination, we collected PBMCs from individuals pre-booster and at 8 days and 4 weeks after booster vaccination. S-specific CD8 T cells were visulaized by using a cocktail of peptide-loaded HLA-A-02 tetramers (to assess CD8 T cell responses to four epitopes restricted by the same MHC). S-specific CD8 T cells were present at low frequencies pre-booster (<0.1%), but at day 8 after booster, S-specific CD8 T cells were detected at high frequencies in 5 of 10 individuals (**Fig. 4D**). At day 8, more than 50% of S-specific CD8 T cells expressed CXCR3, CX3CR1, KLRG1, and PD-1. Further, 50-80% of S-specific CD8 T cells expressed perforin and/or granzyme B, suggestive of effector differentiation (**Fig. 4E**). In the ensuing 3 weeks, there was ~75% reduction in the frequencies of S-specific CD8 T cells, but the levels were significantly above the pre-booster levels (**Fig. 4D**). Like mouse PBMCs, there was a signature of high levels of CXCR3 and CX3CR1 at peak that continued into memory, low levels of CD69 and CD103, stable levels of KLRG1 with increasing levels of CD127 over time, and peak levels of PD-1 that corresponded to recent vaccination (**Fig. 4E**). Thus, overall, the kinetics of the CD8 T cell response to a booster mRNA vaccine in humans and mice were similar (**Fig. 4A** to **4E**).

Lung-Protective Recall CD8 T Cell Responses to SARS-CoV-2 Challenge

Protective immunity afforded by human COVID-19 mRNA vaccines are linked to stimulation of spike-specific virus-neutralizing antibodies, which are expected to ablate infection with a homologous or a cross-reactive SARS-CoV-2 variant. However, we have shown previously that antibodies to the spike protein of the original Washington strain of SARS-CoV-2 failed to neutralize the B.1.351 variant of SARS-CoV-2 in mice (18). To limit the role for antibodies in protection and eliminate the need for K18 human ACE2 transgenic mice, we generated a mouse-adapted SARS-CoV-2 virus (MA-10/B.1.351) with the spike protein from the South African β Variant of SARS-CoV-2 (B.1.351); MA-10 virus replicates to high levels in lungs of unmanipulated C57BL/6 mice (28). Cohorts of mice vaccinated IM with the monovalent COVID-19 mRNA vaccine were challenged with the MA-10/B.1.351 virus. On the 5^{th} day after viral challenge, we assessed viral load in lungs and recall CD8 T cell responses in lungs and mLNs (**Fig. 5A**). Upon viral challenge, vaccinated animals mounted strong recall CD8 T cell responses in lungs and draining lymph nodes (**Fig. 5A**) and reduced viral burden in lungs to levels that were below the level of detection (**Fig. 5A**). Unlike lung effector/memory CD8 T cells that were primarily intravascular and expressed little or no CD103 or CD69 prior to challenge (**Fig. S4C**), following viral challenge, more than 50% of S525-specific CD8 T cells displayed extra-vascular localization, likely to the lung interstitium, and expressed increased levels of CD103 and/or/CD69 (13%), and granzyme B (**Fig. 5B-D**). Likewise, subset of S525-specific CD8 T cells in the lung draining lymph nodes expressed granzyme B (**Fig. 5D**). Lung CD8 T cells expressed effector-driving transcription factors T-bet and/or EOMES, but all S525-specific CD8 T cells in draining lymph nodes were $EOMES^{+ve}$ (**Fig. 5E**). Interestingly, all proliferating ($Ki67^{+ve}$) cells in lungs and lymph nodes expressed high levels of EOMES (**Fig. 5F**). On an average, 30% and 70% of S525-specific CD8 T cells expressed the pro-survival transcription

factor TCF-1 in lungs and lymph nodes, respectively (**Fig. 5D**). Thus, SARS-CoV-2 control in lungs of mRNA vaccinated mice was associated with accumulation of proliferating granzyme B^{+ve} effector CD8 T cells in the extravascular lung tissue. Seven to nine percent of lung CD8 T cells produced IFNγ following ex vivo stimulation with the S525 peptide (**Fig S6**), and the cytokine-producing cell frequencies mirror frequencies of MHC I tetramer^{+ve} S525-specific CD8 T cells (~12%); both vascular and extravascular CD8 T cells expressed IFNγ upon stimulation.

Next, we carefully assessed the kinetics of lung viral control and pulmonary recall CD8 T cell responses at days 1, 3, and 5 after SARS-CoV-2 challenge of vaccinated mice (**Fig. S7**). As shown in **Fig. S7A**, lung viral load in vaccinated mice was ~3 Log_{10} lower than in unvaccinated mice within 1-3 days after viral challenge, and by day 5, infectious virus had been almost completely eliminated in lung. Rapid viral control in lungs was associated with expeditious increase in the frequencies of granzyme B-expressing S525-specific CD8 T cells by day 1 after challenge, as compared to frequencies of memory CD8 T cells (**Fig. 3A**). Strikingly, while almost all memory CD8 T cells are found intravascularly in the lungs prior to challenge (**Fig. S7A**), 40-60% of S525-specific CD8 T cells were found localized to the extravascular tissue within 1-3 days after challenge (**Fig. S7A)**, suggestive of rapid extravasation of vascular memory CD8 T cells into the infected lungs. Furthermore, extravascular but not intravascular S525-specific CD8 T cells in lungs of virally challenged mice displayed CD69 expression, indicative of viral antigen recognition (**Fig. S7B);** CD69 expression was highest at day 1 but tapered off as viral load decreased in the lungs. Consistent with the report that $KLRG1^{HI}$ CD4 T cells have reduced ability to migrate out of the lung vasculature (29), we found higher KLRG1 expression on vascular CD8 T cells and enrichment for $KLRG1^{LO}$ CD8 T cells among the

extravascular S525-specific CD8 T cells in the lungs following viral challenge (**Fig. S7B).** Taken together, data in Fig. S7 suggested that rapid SARS-CoV-2 control in lungs of mRNA vaccinated mice was associated with expeditious accumulation of KLRG1^{LO} granzyme B-expressing effector CD8 T cells in the extravascular lung tissue.

Next, to delineate the role of memory CD4 or CD8 T cells in protection against lung SARS-CoV-2 infection, we vaccinated mice with the monovalent or the bivalent vaccine, and depleted CD4 or CD8 T cells, just prior to a challenge with the MA-10/B.1.351 virus. At day 5 after viral challenge, there were strong recall CD8 T cell responses in lungs of un-depleted and CD4 T cell-depleted vaccinated mice (**Fig. 6A**), but not in CD8 T cell-depleted mice. Note the loss of S525-specific CD8 T cells and activated CD4 T cells in lungs of CD8 T cell-depleted and CD4 T cell-depleted mice, respectively. As shown in **Fig. 6B**, viral burden in lungs of un-depleted vaccinated mice was 5 logs lower than in lungs of un-vaccinated controls. Remarkably, depletion of CD4 or CD8 T cells resulted in loss of viral control and high viral titers in lungs, as compared to un-depleted vaccinated mice. Taken together, these findings demonstrated that memory CD4 and CD8 T cells induced by mRNA vaccination play an essential role in reducing SARS-CoV-2 viral burden in lungs.

The lack of viral control in CD4 T cell depleted mice cannot be explained by diminished frequencies of S-specific CD8 T cells in lungs (**Fig. 6A**). Therefore, next, we hypothesized that memory CD4 T cells promoted SARS-CoV-2 control in lungs by facilitating the extravasation of systemic memory CD8 T cells from the vasculature into the pulmonary interstitium. Intravascular staining demonstrated that >60% of S-specific CD8 T cells in the lungs of un-

depleted virally challenged mice were found in the extravascular pulmonary interstitium (**Fig. 6C**). In striking contrast, in CD4 T cell depleted mice, up to 80% of S-specific CD8 T cells were stalled in the lung vasculature, and interestingly CD4 depletion did not appear to substantially alter expression of either CD69,CD103, CD49a, CX3CR1 or CD44, relative to undepleted mice (**Fig. 6D**); thus expression of molecules that promote tissue residency or trafficking were minimally altered in CD4 T cell-depleted mice (30-33). These data demonstrated the critical importance of CD4 T cells in facilitating memory CD8 T cell extravasation into lung interstitium following viral challenge.

Vaccine-Elicited Splenic Memory CD8 T Cells Traffic to Airways and Control SARS-CoV-2 in Lungs

To reiterate, spike specific CD8 T cells elicited by mRNA vaccination were detected in the lung vasculature, but also unexpectedly to a high degree in the airways (BAL) of mice. It was of interest to determine whether memory CD8 T cells in the airways are descendants of their systemic splenic counterparts. To address this question, at 100 days after vaccination, CD8 T cells (containing 50-100 thousand S525-specific memory CD8 T cells) purified from spleens of CD45.2 vaccinated mice were adoptively transferred into naïve congenic CD45.1 C57BL/6 mice. We confirmed that spleen, BAL, and mLN of donor mice contained S525-specific CD8 T cells that were similar in frequencies and phenotype to those described in Fig 3A **(Fig**. **7A).** Cell recipient mice were euthanized 7 and 30 days after adoptive transfer to examine the tissue distribution and phenotypes of donor memory CD8 T cells. Of great interest, at D7 following transfer, high frequencies of donor CD45.2+/S525+ CD8 T cells were detected in airways of these mice, as measured in BAL (**Fig. 7B**), and these cells persisted to high levels for at least

30 days (**Fig. 7C**). Donor CD45.2+/S525+ CD8 T cells were also readily detected in lungs, mLNs and spleens, at both D7 and D30, and donor memory CD8 T cells localized to the lung vasculature (**Fig. 7B, 7C**). These data suggested that splenic memory CD8 T cells induced by intramuscular mRNA vaccination can migrate and potentially perform immunosurveillance in the airways.

Next, we investigated whether adoptively transferred splenic memory CD8 T cells can reduce SARS-CoV-2 load in lungs. At 100 days after mRNA vaccination, CD8 T cells were purified from spleen and adoptively transferred into congenic CD45.1 mice. Thirty days after adoptive transfer, recipient mice were challenged with the MA-10/B.1.351 virus. At 5 days after challenge, we found elevated numbers of donor CD45.2^{+ve} granzyme B-expressing S525-specific effector CD8 T cells in lungs (**Fig. 7D**). These donor CD8 T cells in lungs also expressed high levels of effector transcription factors EOMES and T-bet. Viral burden in lungs of adoptive transfer recipients was 10-100-fold lower than in un-transferred mice i.e., >90% reduction in viral load (**Fig. 7E**). Thus, splenic memory CD8 T cells significantly *(P*<0.05) reduced SARS-CoV-2 levels in the lungs. Next, we assessed whether mRNA vaccine-elicited memory CD8 T cells persist long-term (Day 232) and retain the ability to protect against SARS-CoV-2 in the lungs. At 232 days after vaccination, in all organs examined, the frequencies and phenotypes of S525-specific memory CD8 T cells were largely comparable to those at 96 days after vaccination, except for an enrichment of central memory (CD62L^{+ve}) phenotype cells and a reduction in the relative proportions of CX3CR1^{+ve} subsets at day 232 (**Fig. S4B-H, Fig S8A, S8B)**. To assess memory CD8 T cell-dependent SARS-CoV-2 control in lungs, we adoptively transferred CD8 T cells purified from spleen of mRNA vaccinated (Day 232) or unvaccinated

mice into C57BL/6 mice, which were challenged with MA-10/B.1.351 virus. Akin to day 100 memory CD8 T cells (**Fig. 7E**), day 232 memory CD8 T cells from vaccinated mice also significantly ($P<0.01$) reduced viral burden in lungs, relative to CD8 T cells from unvaccinated mice (**Fig. S8C)**. These data suggested that mRNA vaccine-elicited splenic memory CD8 T cells provide durable protective immunity to SARS-CoV-2 in the lungs.

DISCUSSION

Several studies have quantified circulating levels of antibody and T cell responses to COVID-19 mRNA vaccines in humans (6-13), but the magnitude and the character of T cell responses in tissues including lungs and lymphoid tissues remain unknown. While a growing body of evidence suggesting that mRNA vaccines can elicit potent cellular responses (6-13), the role of memory CD4 or CD8 T cells in mRNA vaccine-induced protection is unclear. Here, using non-transgenic immunocompetent C57BL/6 mice, we have systematically analyzed the kinetics, phenotype, and tissue distribution of COVID-19 human mRNA vaccine-elicited antigen-specific CD8 T cells, and the role of memory CD4 and CD8 T cells in controlling SARS-CoV-2 replication in the lungs.

The kinetics of CD8 T cell responses to live viral vaccines such as the yellow fever vaccine (YFV) in humans or acute viral infections in mice (e.g. lymphocytic choriomeningitis virus [LCMV]) are comprised of three phases: expansion, contraction, and memory (34, 35). Remarkably our studies show that CD8 T cell responses to the human COVID-19 mRNA vaccine of mice and humans mimicked the kinetics of the CD8 T cell response to acute viral infections in mice and humans. The peak of the CD8 T cell response in mice occurred at days 5-8 after booster mRNA vaccination, and 70-90% of CD8 T cells were lost in spleen, lungs, and lymph nodes during the ensuing contraction phase. The kinetics of CD8 T cells in the circulation mirrored contraction in spleen and lymph nodes. As in acute viral infections (35, 36), longitudinal analysis of CD8 T cell frequencies showed that the frequency at the peak of the response i.e., clonal burst size forecasts the magnitude of CD8 T cell memory, following mRNA

vaccination. Up to ~200 days after vaccination, substantive numbers of CXCR3^{+ve} memory CD8 T cells were detected in all tissues examined including the pulmonary vasculature and lung airways. Further, as in an acute viral infection, the CD8 T cell response to mRNA vaccine in mice is highly potent, and the frequencies of effector CD8 T cells specific to a single epitope reach 10-20% of CD8 T cells in spleen and airways at the peak of the response. The human CD8 T cell responses to COVID-19 mRNA vaccine is robust, but the magnitude appears lower, as compared to those of SPF mice. This discrepancy could be explained by the possibility that we might be underestimating the frequencies of S-specific CD8 T cells in humans because the MHC I tetramer cocktail that we used stains CD8 T cells recognizing epitopes restricted by only one MHC molecule, which likely constitutes a small fraction of all S-specific CD8 T cells elicited in the human vaccinee. Second, it is possible that unlike SPF mice, humans experience diverse microbial exposure throughout their lifetime, which might have dampened the CD8 T cell response to vaccines in humans (37). Therefore, to mimic the diverse microbial exposure of vaccinated humans, mRNA vaccines should be tested in 'Dirty' mice (38) that seem to model human responses more accurately than the SPF mice. However, it is noteworthy that despite the differences in the overall magnitude of the CD8 T cell responses, circulating S-specific CD8 T cells in SPF mice and humans displayed remarkable similarities in the kinetics, cell surface phenotype, and the subset heterogeneity among effector and memory T cells.

Notably, akin to effector CD8 T cells elicited by viral infections, CD8 T cells elicited by the mRNA vaccine differentiated into MPECs or SLECs that displayed traits of bonafide effector cells - expressed granzyme B and T-bet, and produced cytokines such as IFNγ. This is highly significant because T cell responses triggered by acute viral infections result in durable T cell

memory that lasts decades after infection, and vaccinologists have been striving to mimic such T cell programming to elicit long-term immunity (39). The current study evaluated CD8 T cell immunity in mice for only 232 days, but studies of human peripheral blood suggest that T-cell memory induced by human COVID-19 mRNA vaccines is durable (8, 40-42). Mechanistically, the degree and nature of the early inflammatory response plays a crucial role in regulating the development and differentiation of effector and memory T cells following viral or intracellular bacterial infections (43, 44). Taken together, we propose that the COVID-19 mRNA vaccine likely mimics an anti-viral innate inflammatory response that programs the robust differentiation of a heterogeneous pool of Type 1 effector CD8 T cells containing subsets that transition into long-lived memory T cells and display durable persistence in circulation, lymphoid tissues, and lung airways.

Typically, parenteral administration of subunit or inactivated vaccines does not elicit mucosal or tissue-resident T cell immunity (45). Surprisingly, the COVID-19 mRNA vaccine administered into the gastrocnemius muscle in the hind limbs of mice, elicit high numbers of antigen-specific CD8 T cells in spleen, lungs, airways, mLN (non-draining LN) and iLN (draining LN), which is suggestive of a systemic response. The systemic dissemination of effector CD8 T cells might be explained by dispersal of the mRNA vaccine beyond the site of injection to other tissues such as spleen (46). It is also noteworthy that considerable numbers of effector CD8 T cells were found in lungs and airways, the target tissue for SARS-CoV-2. However, it is worth pointing out that the effector CD8 T cells in lungs did not display mucosal imprinting and were found exclusively within the pulmonary vasculature and not in the lung interstitium. Similar to our findings with mice, S-specific CD4 T cells are readily detectable in the lungs of humans

receiving the mRNA vaccine, and such cells do not display markers of tissue residency (47). While these data suggest that effector CD8 T cells in the lung vasculature are unable to trans-endothelially migrate into the lung interstitium, it is unknown why do effector CD8 T cells accumulate in the airways but not traffic to the lung interstitium? The differential migration of effector/memory T cells might be a sequel to the distinct hemodynamic properties and/or the specialized characteristics of the vasculature involved in the regional blood circulation. Blood supply to lungs occur via two different types of circulation: pulmonary circulation and bronchial circulation that supply blood to alveoli and airways, respectively. The pressure in the bronchial artery is 6 times that of the pressure in the pulmonary artery, which might assist CD8 T cells in trans-endothelial migration into airways. The differences in the diameter of blood vessels and expression of adhesion molecules on endothelial cells between the two types of arteries might underlie preferential migration of effector CD8 T cells to the airways but not to the lung interstitium (48, 49). Circulating effector CD8 T cells lack mucosal imprinting (expression of CD103 or CD49a) and therefore might readily egress the lung interstitium but fail to accumulate extravascularly. In concurrence with our findings, S-specific memory CD4 T cells have been reported in the lungs of mRNA vaccinated humans (47). However, another study failed to detect memory CD8 T cells in BAL of humans or mice receiving the COVID-19 mRNA vaccine (50). This discrepancy may be explained by differences in the techniques used to visualize S-specific CD8 T cells. In our study, we used MHC I tetramers to detect CTLs specific to the immunodominant S525 epitope, whereas Tang et al., used the less sensitive functional readout such as cytokine production to identify S-specific CD8 T cells in the BAL. In our experience, a fraction of CD8 T cells in the BAL express PD-1 and are less able to display their functional attributes ex vivo, and hence a less reliable method to identify antigen-specific CD8 T cells.

Although we can't exclude the possibility that differentiation of effectors capable of migrating to the airways is only seen in mice but not in humans, quantification of memory CD8 T cells in airways of vaccinated humans with MHC I tetramers will confirm whether vaccine-elicited memory CD8 T cells provide immune surveillance in the airways. By studying vaccinia virus-infected mice, Harty and his colleagues reported continuous trafficking of systemic $CXCR3^+$ memory CD8 T cells, as a mechanism of maintaining airway memory CD8 T cells (51). They also reported that memory CD8 T cells induced by vaccinia virus were superior to those induced by *Listeria monocytogenes* in trafficking to airways (51). It is possible that the superior trafficking of vaccinia virus-induced memory CD8 T cells to airways is linked to lung/airway virus replication and the associated mucosal programming of CD8 T cells. The persistence of airway memory CD8 T cells especially those induced by intramuscular mRNA vaccination is entirely unexpected. These airway memory CD8 T cells did not express tissue residency markers such as CD103 and CD49a, and less likely to be mucosally programmed driven by dispersal of vaccine mRNA to the respiratory tissues and antigen expression in lungs or airways. Therefore, we favor the hypothesis that airway memory CD8 T cells in mRNA vaccinated mice are descendants of circulating effector memory CD8 T cells. Indeed, we demonstrate that memory CD8 T cells in spleen of mRNA vaccinated mice traffic from the circulation to the airways, survive for at least 30 days, and show excellent protective and recall responses upon viral challenge. Our study provided fundamental insights into the trafficking of circulating memory CD8 T cells into airways, but we did not assess the exclusive role of airway memory CD8 T cells in protection against SARS-CoV-2 infection. Future work will assess whether intratracheal transfer of mRNA vaccine-elicited airway memory CD8 T cells provides protection against challenge with SARS-CoV-2.

Depletion of CD4 or CD8 T cells compromised SARS-CoV-2 control in lungs of mRNA vaccinated mice. The mechanisms underlying the requirement for both CD4 and CD8 T cells in SARS-CoV-2 control might be multifaceted. We find that CD4 T cells promotes extravasation of memory CD8 T cells to SARS-CoV-2-infected lungs, but the underlying mechanisms are unknown and warrant further investigation. Previous work has shown that memory CD8 T cells fail to traffic into infected tissues without CD4 T cells (52); in that report, authors demonstrate that memory CD4 T cells traffic to the virally infected tissue first and produce IFNγ that induce the production of chemokines, and license recruitment of memory CD8 T cells from the circulation in a CXCR3-dependent fashion (52). We find no alterations in the expression of CX3CR1 and CD44 on S525-specific effector CD8 T cells in CD4 T-cell-depleted group following viral challenge, but further studies are warranted to test: (1) the role of CXCR3 in regulating trafficking of CD8 T cells into the lungs; (2) whether the effector functions of CD4 T cells directly mediate viral control in lungs. Additionally, there is a need to investigate mutual interdependence of CD4 and CD8 T cells in SARS-CoV-2 control in lungs, as shown in models of tumor immunity, where APCs in the tumor environment are required to co-activate CD4 and CD8 T cells to reduce tumor burden (53, 54).

While several studies have documented durable T cell responses following mRNA vaccination (8, 40-42), recent work from the Davis group show that mRNA vaccine stimulate high numbers of CD8 CTLs and such CTLs are superior to those induced by the SARS-CoV-2 infection (55). Another study showed that breakthrough SARS-CoV-2 infections elicit rapid recall responses of both CD4 and CD8 T cells and the magnitude of CD8 T cell activation correlates with the

rate of viral control (56). These data strongly suggest a role for CD8 T cells in viral control following breakthrough infections, but mechanistic experiments to assess the precise role of T cells in protection against SARS-CoV-2 in lungs in humans are challenging to do. Additionally, data from such studies are difficult to interpret, especially because of comorbidities and other confounding variables prevalent in the human population. In this context, by performing T cell depletion experiments in vaccinated mice and by adoptive transfer of memory CD8 T cells into naïve mice, our study provides unequivocal evidence that mRNA vaccine elicited memory CD8 T cells are necessary and sufficient to effectively limit replication of a SARS-CoV-2 in lungs. We document that the rapid extravascular accumulation of memory CD8 T cells and their CD4 T cell-dependent migration into lungs was associated with expeditious SARS-CoV-2 control, but a major limitation of our study is that we did not exclude the role of binding and/or neutralizing antibodies in lung viral control. It is likely that rapid migration of vascular memory T cells into infected lungs is one of many immunological mechanisms that reduce disease severity, and lower hospitalizations in human vaccinees infected with antibody evasive viral variants (57-59). It is paradigmatic that resident memory T cells in the airways and lungs provide constitutive immunity at mucosal barriers without the need for T cell migration from the systemic circulation. In our study, intramuscular mRNA vaccination did not induce classical mucosally imprinted resident memory T cells in the airways or the lungs, and this finding is consistent with a human study that failed to detect resident memory T cells in the nose, following mRNA vaccination (60). However, following viral challenge, we find increased frequencies of virus-specific CD8 T cells in the lungs that expressed tissue residency markers such as CD103. These data suggest that systemic memory T cells induced by mRNA vaccine can potentially differentiate into resident memory following breakthrough infections. Indeed,

this interpretation is supported by a report that show development of naso-pharynx or nasal-resident memory T cells following breakthrough infection in humans (60, 61). Another limitation of our study is that we did not assess memory T cells in nose and upper respiratory tract or their role in controlling viral replication and/or transmission. It will be important to assess the biological significance of nasal and airway resident memory T cells in protection against emerging variants of SARS-CoV-2. Addressing this issue is of fundamental importance because we still do not know whether individuals that recover from breakthrough SARS-CoV-2 infections require further vaccinations or that the 'hybrid immunity' is sufficient to provide broad mutation resistant immunity to future SARS-CoV-2 variants.

In summary, in this manuscript, we document that the human COVID-19 mRNA vaccine stimulated highly potent systemic CD8 T cell responses in humans and mice, and the magnitude of the response rivaled the exuberant CD8 T cell responses seen in acute viral infections. We show that vaccine-elicited memory CD8 T cells home to the pulmonary vasculature, lung draining lymph nodes and airways, and potentially perform regional immunosurveillance in the respiratory tract. Significantly, we find that memory CD8 T cells are necessary and sufficient to limit SARS-CoV-2 replication in lungs. In summary, our studies highlight the non-redundant functiion of memory CD8 T cells in protection against SARS-CoV-2, and ascribes a prominent role for memory T cells in limiting severe disease and hospitalization following breakthrough infections.

MATERIAL AND METHODS

Experimental Animals

Seven-to-twelve-week-old male and female C57BL/6J (B6) were purchased from the Jackson Laboratory (Bar Harbor, ME, USA).

Reagents

Reagents used in these studies are listed in Supplemental Methods and in Supplemental Table 1.

Vaccination

The Pfizer-BioNTech monovalent (BNT162b2 [Original]) or the bivalent vaccines (or BNT162b2 [Original/Omicron BA.4/BA.5]) were provided by the University of Wisconsin Hospitals. The mRNA vaccinations were administered intramuscularly (100μL) into the gastrocnemius muscle. In some experiments, mice were anaesthetized with isoflurane and vaccinated intranasally (50 μL). All mice were vaccinated twice at an interval of 3 weeks.

Tissue Processing, Flow Cytometry and Ex vivo Cytokine Analysis

BAL, Lymph nodes, spleens and lungs harvested at necropsy were processed into single cell suspensions and stained for cellular factors, as previously described (62) and in Supplemental Methods, or used in western blot assays**.** For western blot assays, primary antibodies used were anti- β-actin (Cell Signaling technology, mouse mAb, clone 8H10D10, 1:4000 dilution) and anti-TCF-1 (Cell Signaling technology, rabbit mAb, clone C63D9, 1:1000 dilution).

Cells and Viruses

The MA-10/B.1.351 virus was derived by reverse genetics as described previously (28). Briefly, the SARS-CoV-2 MA10/B.1.351 virus was derived from an infectious clone of SARS-CoV-2

MA10 genetically engineered to replace the mouse adapted WA spike with the native spike from the B.1.351 virus, which can bind to mouse ACE2 receptor. Viruses were cultured and tittered as described in Supplemental Methods**.**

Viral Challenge and Adoptive Cell Transfer

To induce MA-10/B.1.351 SARS-CoV-2 infection, mice were infected with $1x10^4$ PFU by the IN route. Recall responses and viral titers were assessed by euthanizing mice 5 days after infection. To assess the role of CD4 T cells and CD8 T cells in protective immunity, mice were administered 200 μg of anti-CD4 (Bio X Cell, Clone: GK1.5) or anti-CD8 antibodies (Bio X Cell; Clone 2.43) intravenously and intranasally at days -5. -3, -1 and 1, 3, and 5, relative to challenge as indicated. For adoptive transfer studies, spleens were harvested from CD45.2 vaccinated mice at the indicated time post vaccination, processed into single cell suspensions, then enriched for CD8 T cells using a negative selection kit (Miltenyi, 130-104-075). Four to five million CD8 T cells purified from spleens of CD45.2 mRNA vaccinated mice (Purity >90%) were transferred to congenic CD45.1 mice by retro-orbital intravenous injection.

Human Clinical Samples

After informed consent was obtained, peripheral blood was collected from COVID-19 vaccinees prior to the third vaccination, 8 days after the third vaccination, and 4 weeks after the third vaccination. Detailed information of human samples is described in Table 1.

Analysis of Human Samples.

Peripheral blood mononuclear cells (PBMCs) were isolated from blood obtained from COVID-19 vaccinees by using Leucosep Tubes with Porous Barrier (Greiner Bio-One). Cells were then

incubated with Ghost Dye™ Red 780 (Cytek Biosciences) and stained with cocktail of HLA-A*02:01 tetramers (specific to following epitopes in the S protein: 61-70, 222-230, 269-277, and 1000-1008) and antibodies specific to human CD4 (SK3), CD8 (RPA-T8), CD45RA (HI100), CD45RO (UCHL1), HLA-DR (L243), CXCR3 (1C6/CXCR3), CD69 (FN50), PD1 (EH12.2H7), CX3CR1 (2A9-1), CD103 (B-Ly7), CCR7 (3D12), CD56 (HCD56), KLRG1 (14C2A07) and CD127 (HIL-7R-M21) from Biolegend, cell signaling, Becton Dickinson or eBioscience (San Diego, CA, USA). Antibodies against Granzyme B (QA18A28) and Perforin (dG9) were used for intracellular staining using the eBioscience™ Foxp3/Transcription Factor Staining Buffer Set (eBioscience). Data were acquired with CytoFLEX S (Beckman Coulter Inc., Brea, CA, USA) and data analysis was performed using FlowJo software (FlowJo, Ashland, OR USA).

Statistical Analyses

Statistical analyses were performed using GraphPad software 9.0 (La Jolla, CA). Planned comparisons were made using a one-way ordinary ANOVA test with multiple comparisons (Fisher's least significant difference test, Fisher's LSD) in group comparisons that did not have signifigantly different standard deviations as determined by Brown-Forsythe and Bartlett's tests, and if signifigantly different, multiple comparisons were made using a Brown-Forsythe and Welch test. Two way comparisons were made using an unpaired t test. *, **, ***, and **** indicate significance at $P<0.05$, 0.005, 0.0005 and 0.00005 respectively. Data in each graph indicate mean ± SEM.

Study approval

All experiments were reviewed and approved by the University of Wisconsin School of Veterinary Medicine Animal Use and Care Committee. For human studies, the research protocol was approved by the Research Ethics Review Committee of the Institute of Medical Science of the University of Tokyo (approval numbers: 2020-74-0226).

Data Availability

Data is made available upon request and all data within graphs is contained with in the attached “supporting data” spreadsheet.

Acknowledgements

We thank the Emory NIH Tetramer Core Facility for providing MHC-I tetramers. We also thank the efforts of the veterinary and animal care staff at UW-Madison. We thankfully acknowledge Amulya Suresh for making the graphical abstract.

Funding

This work was supported by PHS grant U01 AI124299, R21 AI149793-01A1, R21 AI173757-01A1 and John E. Butler professorship to M. Suresh.

Author Contributions

BB, TC, HB, HP, RU, BY, JM, and MS designed, performed, and analyzed experiments

PH provided critical reagents and assisted with experimental planning

KI-H, MK, SY, and HY contributed to collection and preparation of human clinical samples

BB and MS wrote the manuscript, which was proofread by all authors

SK, RB and YK provided conceptual input and mentored researchers in their laboratories

Co-first authorship and authorship order was determined by the contributions of the two authors to concept development, experimentation, data collection and analysis, and manuscript preparation.

Bibliography

1. Tenforde MW, Link-Gelles R, and Patel MM. Long-term Protection Associated With COVID-19 Vaccination and Prior Infection. *JAMA.* 2022;328(14):1402-4.
2. Lin D-Y, Gu Y, Xu Y, Wheeler B, Young H, Sunny SK, et al. Association of Primary and Booster Vaccination and Prior Infection With SARS-CoV-2 Infection and Severe COVID-19 Outcomes. *JAMA.* 2022;328(14):1415-26.
3. Lin D-Y, Gu Y, Wheeler B, Young H, Holloway S, Sunny S-K, et al. Effectiveness of Covid-19 Vaccines over a 9-Month Period in North Carolina. *New England Journal of Medicine.* 2022;386(10):933-41.
4. Lauring AS, Tenforde MW, Chappell JD, Gaglani M, Ginde AA, McNeal T, et al. Clinical severity of, and effectiveness of mRNA vaccines against, covid-19 from omicron, delta, and alpha SARS-CoV-2 variants in the United States: prospective observational study. *BMJ.* 2022;376:e069761.
5. Tarke A, Coelho CH, Zhang Z, Dan JM, Yu ED, Methot N, et al. SARS-CoV-2 vaccination induces immunological T cell memory able to cross-recognize variants from Alpha to Omicron. *Cell.* 2022;185(5):847-59.e11.
6. Gao F, Mallajoysula V, Arunachalam PS, van der Ploeg K, Manohar M, Röltgen K, et al. Spheromers reveal robust T cell responses to the Pfizer/BioNTech vaccine and attenuated peripheral CD8⁺ T cell responses post SARS-CoV-2 infection. *Immunity.* 2023;56(4):864-78.e4.
7. Zhang Z, Mateus J, Coelho CH, Dan JM, Moderbacher CR, Gálvez RI, et al. Humoral and cellular immune memory to four COVID-19 vaccines. *Cell.* 2022;185(14):2434-51.e17.
8. Goel RR, Painter MM, Apostolidis SA, Mathew D, Meng W, Rosenfeld AM, et al. mRNA vaccines induce durable immune memory to SARS-CoV-2 and variants of concern. *Science.* 2021;374(6572):abm0829.
9. Sahin U, Muik A, Vogler I, Derhovanessian E, Kranz LM, Vormehr M, et al. BNT162b2 vaccine induces neutralizing antibodies and poly-specific T cells in humans. *Nature.* 2021;595(7868):572-7.
10. Oberhardt V, Luxenburger H, Kemming J, Schulien I, Ciminski K, Giese S, et al. Rapid and stable mobilization of CD8+ T cells by SARS-CoV-2 mRNA vaccine. *Nature.* 2021;597(7875):268-73.
11. McMahan K, Yu J, Mercado NB, Loos C, Tostanoski LH, Chandrashekar A, et al. Correlates of protection against SARS-CoV-2 in rhesus macaques. *Nature.* 2021;590(7847):630-4.
12. Mallajosyula V, Ganjavi C, Chakraborty S, McSween AM, Pavlovitch-Bedzyk AJ, Wilhelmy J, et al. CD8⁺ T cells specific for conserved coronavirus epitopes correlate with milder disease in patients with COVID-19. *Science Immunology.* 2021;6(61):eabg5669.
13. Tang J, Zeng C, Cox TM, Li C, Son YM, Cheon IS, et al. Respiratory mucosal immunity against SARS-CoV-2 after mRNA vaccination. *Science Immunology.* 2022;7(76):eadd4853.
14. Gebre MS, Rauch S, Roth N, Gergen J, Yu J, Liu X, et al. mRNA vaccines induce rapid antibody responses in mice. *npj Vaccines.* 2022;7(1):88.
15. Chen Y, Song W, Li C, Wang J, Liu F, Ye Z, et al. COVID-19 mRNA vaccine protects against SARS-CoV-2 Omicron BA.1 infection in diet-induced obese mice through boosting host innate antiviral responses. *EBioMedicine.* 2023;89:104485.

16. Garcia-Dominguez D, Henry C, Ma L, Jani H, Amato NJ, Manning T, et al. Altering the mRNA-1273 dosing interval impacts the kinetics, quality, and magnitude of immune responses in mice. *Frontiers in Immunology.* 2022;13.
17. Liu J, Budylowski P, Samson R, Griffin BD, Babuadze G, Rathod B, et al. Preclinical evaluation of a SARS-CoV-2 mRNA vaccine PTX-COVID19-B. *Science Advances.* 2022;8(3):eabj9815.
18. Kingstad-Bakke B, Lee W, Chandrasekar SS, Gasper DJ, Salas-Quinchucua C, Cleven T, et al. Vaccine-induced systemic and mucosal T cell immunity to SARS-CoV-2 viral variants. *Proc Natl Acad Sci U S A.* 2022;119(20):e2118312119.
19. Zhang J, Lyu T, Cao Y, and Feng H. Role of TCF-1 in differentiation, exhaustion, and memory of CD8+ T cells: A review. *The FASEB Journal.* 2021;35(5):e21549.
20. Gerlach C, Moseman EA, Loughhead SM, Alvarez D, Zwijnenburg AJ, Waanders L, et al. The Chemokine Receptor CX3CR1 Defines Three Antigen-Experienced CD8 T Cell Subsets with Distinct Roles in Immune Surveillance and Homeostasis. *Immunity.* 2016;45(6):1270-84.
21. Buchholz VR, and Busch DH. Back to the Future: Effector Fate during T Cell Exhaustion. *Immunity.* 2019;51(6):970-2.
22. Kurhade C, Zou J, Xia H, Liu M, Chang HC, Ren P, et al. Low neutralization of SARS-CoV-2 Omicron BA.2.75.2, BQ.1.1 and XBB.1 by parental mRNA vaccine or a BA.5 bivalent booster. *Nature Medicine.* 2023;29(2):344-7.
23. Jacobsen H, Strengert M, Maaß H, Ynga Durand MA, Katzmarzyk M, Kessel B, et al. Diminished neutralization responses towards SARS-CoV-2 Omicron VoC after mRNA or vector-based COVID-19 vaccinations. *Scientific Reports.* 2022;12(1):19858.
24. Lyke KE, Atmar RL, Islas CD, Posavad CM, Szydlo D, Paul Chourdhury R, et al. Rapid decline in vaccine-boosted neutralizing antibodies against SARS-CoV-2 Omicron variant. *Cell Reports Medicine.* 2022;3(7).
25. Tada T, Zhou H, Dcosta BM, Samanovic MI, Chivukula V, Herati RS, et al. Increased resistance of SARS-CoV-2 Omicron variant to neutralization by vaccine-elicited and therapeutic antibodies. *eBioMedicine.* 2022;78.
26. Groom JR, and Luster AD. CXCR3 ligands: redundant, collaborative and antagonistic functions. *Immunology & Cell Biology.* 2011;89(2):207-15.
27. Lord GM, Rao RM, Choe H, Sullivan BM, Lichtman AH, Luscinskas FW, et al. T-bet is required for optimal proinflammatory CD4+ T-cell trafficking. *Blood.* 2005;106(10):3432-9.
28. Leist SR, Dinnon KH, Schäfer A, Tse LV, Okuda K, Hou YJ, et al. A Mouse-Adapted SARS-CoV-2 Induces Acute Lung Injury and Mortality in Standard Laboratory Mice. *Cell.* 2020;183(4):1070-85.e12.
29. Sakai S, Kauffman KD, Schenkel JM, McBerry CC, Mayer-Barber KD, Masopust D, et al. Cutting edge: control of Mycobacterium tuberculosis infection by a subset of lung parenchyma-homing CD4 T cells. *J Immunol.* 2014;192(7):2965-9.
30. Masopust D, and Soerens AG. Tissue-Resident T Cells and Other Resident Leukocytes. *Annu Rev Immunol.* 2019;37:521-46.
31. Combadière B, Faure S, Autran B, Debré P, and Combadière C. The chemokine receptor CX3CR1 controls homing and anti-viral potencies of CD8 effector-memory T lymphocytes in HIV-infected patients. *AIDS.* 2003;17(9):1279-90.

32. Siddiqui I, Erreni M, Brakel Mv, Debets R, and Allavena P. Enhanced recruitment of genetically modified CX3CR1-positive human T cells into Fractalkine/CX3CL1 expressing tumors: importance of the chemokine gradient. *Journal for ImmunoTherapy of Cancer.* 2016;4(1):21.
33. Ponta H, Sherman L, and Herrlich PA. CD44: From adhesion molecules to signalling regulators. *Nature Reviews Molecular Cell Biology.* 2003;4(1):33-45.
34. Akondy RS, Monson ND, Miller JD, Edupuganti S, Teuwen D, Wu H, et al. The yellow fever virus vaccine induces a broad and polyfunctional human memory CD8+ T cell response. *J Immunol.* 2009;183(12):7919-30.
35. Murali-Krishna K, Altman JD, Suresh M, Sourdive DJD, Zajac AJ, Miller JD, et al. Counting Antigen-Specific CD8 T Cells: A Reevaluation of Bystander Activation during Viral Infection. *Immunity.* 1998;8(2):177-87.
36. Hou S, Hyland L, Ryan KW, Portner A, and Doherty PC. Virus-specific CD8+ T-cell memory determined by clonal burst size. *Nature.* 1994;369(6482):652-4.
37. Fiege JK, Block KE, Pierson MJ, Nanda H, Shepherd FK, Mickelson CK, et al. Mice with diverse microbial exposure histories as a model for preclinical vaccine testing. *Cell Host Microbe.* 2021;29(12):1815-27.e6.
38. Li Y, and Baldridge MT. Modelling human immune responses using microbial exposures in rodents. *Nature Microbiology.* 2023;8(3):363-6.
39. Kaech SM, Wherry EJ, and Ahmed R. Effector and memory T-cell differentiation: implications for vaccine development. *Nature Reviews Immunology.* 2002;2(4):251-62.
40. Kuse N, Zhang Y, Chikata T, Nguyen HT, Oka S, Gatanaga H, et al. Long-term memory CD8+ T cells specific for SARS-CoV-2 in individuals who received the BNT162b2 mRNA vaccine. *Nature Communications.* 2022;13(1):5251.
41. Hurme A, Jalkanen P, Heroum J, Liedes O, Vara S, Melin M, et al. Long-Lasting T Cell Responses in BNT162b2 COVID-19 mRNA Vaccinees and COVID-19 Convalescent Patients. *Front Immunol.* 2022;13:869990.
42. Sette A, and Crotty S. Immunological memory to SARS-CoV-2 infection and COVID-19 vaccines. *Immunol Rev.* 2022;310(1):27-46.
43. Butler NS, and Harty JT. The role of inflammation in the generation and maintenance of memory T cells. *Adv Exp Med Biol.* 2010;684:42-56.
44. Jameson SC, and Masopust D. Understanding Subset Diversity in T Cell Memory. *Immunity.* 2018;48(2):214-26.
45. Gasper DJ, Neldner B, Plisch EH, Rustom H, Carrow E, Imai H, et al. Effective Respiratory CD8 T-Cell Immunity to Influenza Virus Induced by Intranasal Carbomer-Lecithin-Adjuvanted Non-replicating Vaccines. *PLoS Pathog.* 2016;12(12):e1006064.
46. Bahl K, Senn JJ, Yuzhakov O, Bulychev A, Brito LA, Hassett KJ, et al. Preclinical and Clinical Demonstration of Immunogenicity by mRNA Vaccines against H10N8 and H7N9 Influenza Viruses. *Mol Ther.* 2017;25(6):1316-27.
47. Pieren DKJ, Kuguel SG, Rosado J, Robles AG, Rey-Cano J, Mancebo C, et al. Limited induction of polyfunctional lung-resident memory T cells against SARS-CoV-2 by mRNA vaccination compared to infection. *Nature Communications.* 2023;14(1):1887.
48. Doerschuk CM. Leukocyte trafficking in alveoli and airway passages. *Respir Res.* 2000;1(3):136-40.

49. Alon R, Sportiello M, Kozlovski S, Kumar A, Reilly EC, Zarbock A, et al. Leukocyte trafficking to the lungs and beyond: lessons from influenza for COVID-19. *Nature Reviews Immunology.* 2021;21(1):49-64.
50. Tang J, Zeng C, Cox TM, Li C, Son YM, Cheon IS, et al. Respiratory mucosal immunity against SARS-CoV-2 after mRNA vaccination. *Sci Immunol.* 2022;7(76):eadd4853.
51. Slütter B, Pewe LL, Kaech SM, and Harty JT. Lung airway-surveilling CXCR3(hi) memory CD8(+) T cells are critical for protection against influenza A virus. *Immunity.* 2013;39(5):939-48.
52. Nakanishi Y, Lu B, Gerard C, and Iwasaki A. CD8(+) T lymphocyte mobilization to virus-infected tissue requires CD4(+) T-cell help. *Nature.* 2009;462(7272):510-3.
53. Ostroumov D, Fekete-Drimusz N, Saborowski M, Kühnel F, and Woller N. CD4 and CD8 T lymphocyte interplay in controlling tumor growth. *Cellular and Molecular Life Sciences.* 2018;75(4):689-713.
54. Wong SBJ, Bos R, and Sherman LA. Tumor-Specific CD4+ T Cells Render the Tumor Environment Permissive for Infiltration by Low-Avidity CD8+ T Cells1. *The Journal of Immunology.* 2008;180(5):3122-31.
55. Gao F, Mallajoysula V, Arunachalam PS, van der Ploeg K, Manohar M, Röltgen K, et al. Spheromers reveal robust T cell responses to the Pfizer/BioNTech vaccine and attenuated peripheral CD8(+) T cell responses post SARS-CoV-2 infection. *Immunity.* 2023;56(4):864-78.e4.
56. Koutsakos M, Reynaldi A, Lee WS, Nguyen J, Amarasena T, Taiaroa G, et al. SARS-CoV-2 breakthrough infection induces rapid memory and de novo T cell responses. *Immunity.* 2023;56(4):879-92.e4.
57. Liu J, Yu J, McMahan K, Jacob-Dolan C, He X, Giffin V, et al. CD8 T cells contribute to vaccine protection against SARS-CoV-2 in macaques. *Science Immunology.* 2022;7(77):eabq7647.
58. Moss P. The T cell immune response against SARS-CoV-2. *Nature Immunology.* 2022;23(2):186-93.
59. Wherry EJ, and Barouch DH. T cell immunity to COVID-19 vaccines. *Science.* 2022;377(6608):821-2.
60. Lim JME, Tan AT, Le Bert N, Hang SK, Low JGH, and Bertoletti A. SARS-CoV-2 breakthrough infection in vaccinees induces virus-specific nasal-resident CD8+ and CD4+ T cells of broad specificity. *Journal of Experimental Medicine.* 2022;219(10).
61. Neidleman J, Luo X, McGregor M, Xie G, Murray V, Greene WC, et al. mRNA vaccine-induced T cells respond identically to SARS-CoV-2 variants of concern but differ in longevity and homing properties depending on prior infection status. *Elife.* 2021;10.
62. Marinaik CB, Kingstad-Bakke B, Lee W, Hatta M, Sonsalla M, Larsen A, et al. Programming Multifaceted Pulmonary T Cell Immunity by Combination Adjuvants. *Cell Rep Med.* 2020;1(6):100095.

Table 1. Information of human samples in this study. All study participants were healthy volunteers of Japanese descent.

ID	Gender	Age
HP(H)- 181	M	53
HP(H)- 182	F	51
HP(H)- 193	M	42
HP(H)- 197	F	58
HP(H)- 221	F	55

Figure Legends

Figure 1. Peak CD8 T cell responses elicited by mRNA vaccination. Mice (n = 6) were administered twice with the BioNTech® mRNA vaccine and euthanized at D5 or D8 after the booster vaccination. Single-cell suspensions of BAL, lungs, spleen, mediastinal or inguinal lymph nodes were stained with viability dye, followed by K^b/S525 (VNFNFNGL) tetramers in combination with antibodies to CD4, CD8, CD44, CD127, KLRG1. (A) Frequencies among CD8 T cells and numbers of S525-specific CD8 T cells in the indicated tissue are shown in FACS plots and graphs at D5 and D8 after booster vaccination. (B, D) FACS plots and graphs show percentages of indicated subsets among $S525^+$ $CD8^+$ T cells in various tissues. (C) To identify circulating/vascular cells in the lungs, mice were injected intravenously with fluorescent-labeled anti-CD45.2 antibodies, 3 min prior to euthanasia ($CD45.2^{+ve}$ – vascular; $CD45.2^{-ve}$ – non-vascular). C shows percentages of vascular ($CD45.2^{+ve}$) and non-vascular ($CD45.2^{-ve}$) cells among S525-specific CD8 T cells. Data represent four independent experiments. Planned comparisons were made using unpaired t test for two-way comparisons (A, C) or Fisher's LSD test (B, D). *, **, ***, and **** indicate significance at $P<0.05$, 0.005, 0.0005 and 0.00005 respectively. Data in each graph indicate mean ± SEM.

Figure 2. mRNA vaccine-elicited effector CD8 T cells are marked by high CXCR3 and granzyme B expression. C57BL/6 mice (n = 6) were vaccinated twice with monovalent BioNTech® mRNA vaccine, euthanized and cells isolated from various tissues were stained as described in Fig. 1, with additional antibodies to granzyme B, TCF-1, CXCR3, CX3CR1, TBET, EOMES, and PD-1. (A-C) FACS plots and graphs show percentages of indicated subsets among $S525^+$ $CD8^+$ T cells in various tissues at days 5 and 8 after boost. Planned comparisons were Fisher's LSD test. *, **, ***, and **** indicate significance at $P<0.05$, 0.005, 0.0005 and 0.00005 respectively. Data in each graph indicate mean ± SEM.

Figure 3. mRNA vaccine-induced mucosal and systemic CD8 T-cell memory. C57BL/6 mice (n = 6) were vaccinated twice with monovalent BioNTech® mRNA vaccine as described in Fig. 1. At 96 days after booster vaccination, S525-specific memory CD8 T cells were characterized in airways (BAL), lungs, spleen, mediastinal (mLN) and inguinal (iLN) lymph nodes. Following euthanasia, organs were collected, and single-cell suspensions were stained with K^b/S525 tetramers and antibodies for the indicated cell surface/intracellular molecules or transcription factors. (A) FACS plots and graphs display percentages or numbers of S525-specific CD8 T cells in various tissues. (B-F) FACS plots are gated on H-2K^b/S525 tetramer-binding cells, and the numbers are the percentages of subsets among the gated population. Data represent two independent experiments. Planned comparisons were made using Fisher's LSD tests. *, **, ***, and **** indicate significance at $P<0.05$, 0.005, 0.0005 and 0.00005. Data in each graph indicate mean ± SEM.

Figure 4. Longitudinal analysis of the kinetics and phenotypes of spike-specific CD8+ T cells in mouse and human PBMCs following administration of the mRNA vaccine. C57BL/6 mice (n = 8) were vaccinated twice with monovalent BioNTech® mRNA vaccine as described in Fig. 1. Human volunteers (n = 5) previously vaccinated with a course of the monovalent mRNA spike vaccine were given a booster of the monovalent BioNTech® mRNA vaccine 180 days later. At the indicated time points before and after vaccination, peripheral blood was collected from mice or humans, and mononuclear cells were stained with K^b/S525 tetramer (mice) or a cocktail of HLA-A*02:01 tetramers (specific to following epitopes in the S protein: 61-70, 222-230, 269-277, and 1000-1008), and antibodies to the indicated cell surface or intracellular molecules. (A, D) Graphs show longitudinal analysis of frequencies of H-2K^b/S525-specific (mice, A) or S-specific (humans, C) tetramer-binding cells among $CD8^+$ T cells in PBMCs of individual mouse or humans. (B, C, E) Percentages of S-specific CD8 T cells expressing the indicated molecule(s) in PBMCs of mice (B, C) or humans (E). Data are from two independent experiments. Planned comparisons were made using Fisher's LSD tests. *, **, ***, and **** indicate significance at $P<0.05$, 0.005, 0.0005 and 0.00005. Data in each graph indicate mean ± SEM.

Figure 5. mRNA vaccine-induced T-cell-dependent protective immunity to a mouse-adapted strain of SARS-CoV-2. Cohorts of 6-8-week-old mice (n=8) were vaccinated twice with BioNTech® mRNA vaccine, as described in Fig 1. At 100 days after booster vaccination, mice were challenged with the MA10/B.1.351 mouse-adapted strain of SARS-CoV-2 virus; unvaccinated mice were challenged as controls. (A) Viral titers and S525-specific CD8 T cells were quantified in the lungs on day 5 after challenge. (B) Percentages of vascular ($CD45.2^+$) or non-vascular ($CD45.2^-$) cells among K^b/S525-specific CD8 T cells in lungs. (C-F) FACS plots are gated on K^b/S525 tetramer-binding CD8 T cells, and the numbers are the percentages of tetramer-binding CD8 T cells within the gate or the quadrant. Two-way comparisons were made using an unpaired t test. *, **, ***, and **** indicate significance at $P<0.05$, 0.005, 0.0005 and 0.00005 respectively. Data in each graph indicate mean ± SEM.

Figure 6. CD8 and CD4 T cells are necessary for mRNA vaccine-induced protective immunity to SARS-CoV-2 in lungs. Cohorts of 6-8-week-old B6 mice (n=5-8) were vaccinated twice with the BioNTech® monovalent (mono) or the bivalent (bi) mRNA vaccine, as described in Fig 1. At 160 days after booster vaccination, mice were treated intranasally and intravenously with anti-CD4 or anti-CD8 antibodies before and during challenge with the MA10/B.1.351 strain of SARS-CoV-2. On the day 5 after viral challenge, lung cells were stained with K^b/S525 tetramers and antibodies to CD8, CD4 and CD44. (A) FACS plots are gated on total CD8 T cells. Graphs in A show number of S525-specific $CD8^+$ and activated ($CD44^+$) CD4 T cells in lungs on day 5 after challenge. (B) Graph shows SARS-CoV-2 titers in lungs. (C) Graph shows percentages of K^b/S525-specific CD8 T cells that were found in the lung vasculature or (D) expressed CD69, CD103, CD49a, CD44 or CX3CR1 in lungs of virally challenged mice. Planned comparisons were made using Fisher's LSD (A, C-D) or Brown-Forsythe and Welch tests (B). *, **, ***, and **** indicate significance at $P<0.05$, 0.005, 0.0005 and 0.00005 respectively.

Figure 7. Vaccine-elicited splenic memory CD8 T cells localize to airways and lymphoid tissues, and protect against SARS-CoV-2 in lungs. Cohorts of 6-8-week-old CD45.2$^+$ C57BL/6 mice (n = 5-10) were vaccinated twice with BioNTech® mRNA vaccine, as described in Fig 1. (A) At 100 days after booster vaccination, frequencies of K^b/S525-specific CD8 T cells were quantified in spleens, LNs and BAL by flow cytometry; FACS plots are gated on total CD8 T cells. (B, C) CD8 T cells purified from spleens of vaccinated mice (from A) were adoptively transferred into congenic CD45.1 mice (n = 4-5). At 8 (B) and 30 (C) days after adoptive cell transfer, the frequencies and phenotype of donor CD45.2$^+$ K^b/S525-specific CD8 T cells in spleen, lymph nodes, lung and BAL were quantified by flow cytometry. FACS plots in B and C are gated on CD45.2$^+$ CD8 T cells. (D, E) At 45 days after adoptive cell transfer, mice were challenged with the MA10/B.1.351 mouse adapted strain of SARS-CoV-2 virus; unvaccinated mice were challenged as controls. (D) On the 5th day after viral challenge, the K^b/S525-specific CD8 T cells in lungs were analyzed by flow cytometry. FACS plots are gated on donor CD45.2$^+$ CD8 T cells. (E) Graph show viral titers in lungs of mice that received memory CD8 T cells (CD8 Transferred) or mice that did not receive any cells (Un-transferred). Planned comparisons were made using Fisher's LSD (A-D), or unpaired t tests (B, C - Thy1.2+ Vascular, E) for two-way comparisons. *, **, ***, and **** indicate significance at P<0.05, 0.005, 0.0005 and 0.00005 respectively. Data in each graph indicate mean ± SEM.

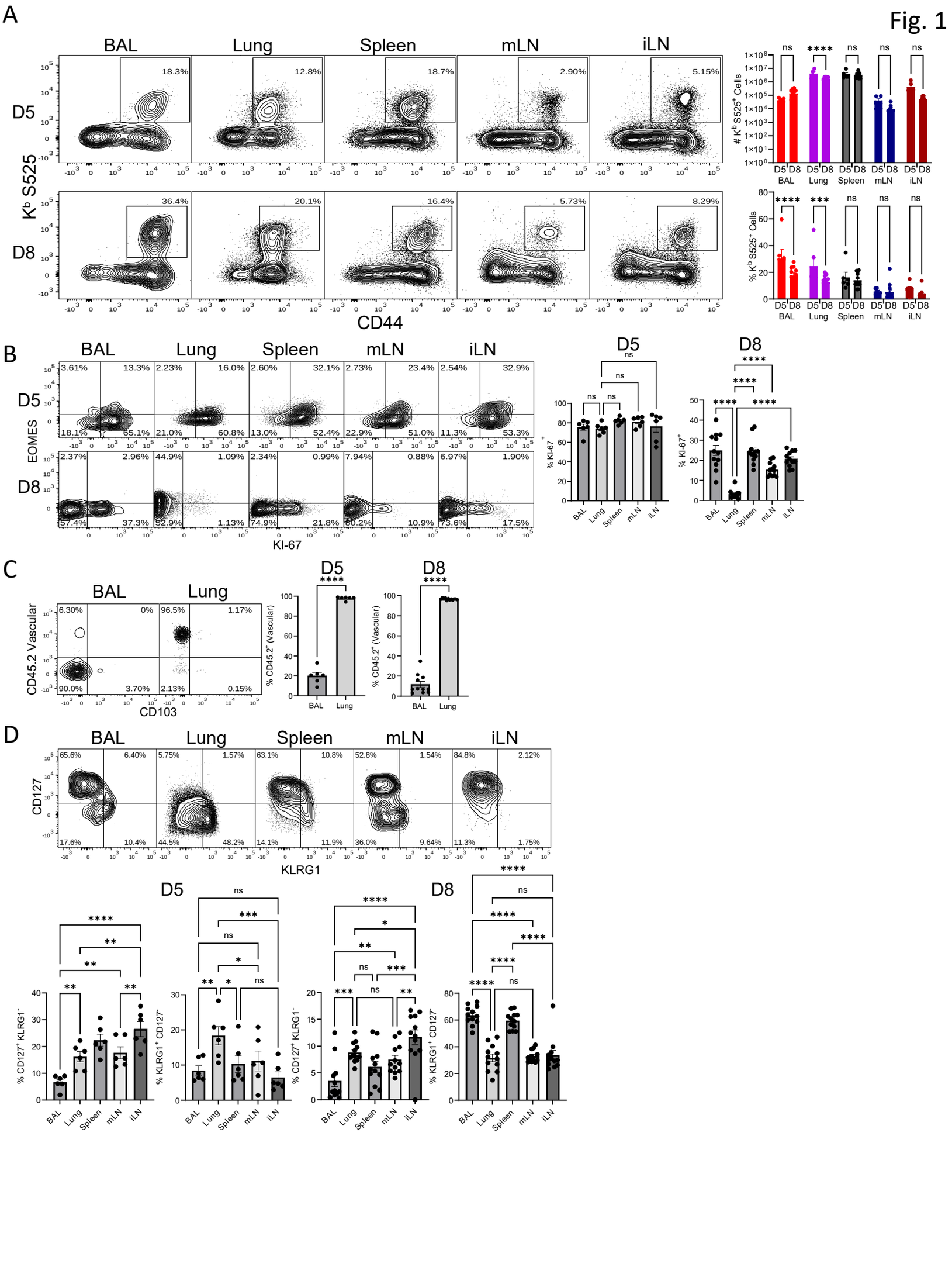
A
BAL
Lung
Spleen
mLN
iLN
D5
D8
Kb S525
CD44
18.3%
12.8%
18.7%
2.90%
5.15%
36.4%
20.1%
16.4%
5.73%
8.29%
Kb S525+ Cells
% Kb S525+ Cells
ns
****
***
D5 D8
B
EOMES
KI-67
3.61%
13.3%
2.23%
16.0%
2.60%
32.1%
2.73%
23.4%
2.54%
32.9%
18.1%
65.1%
21.0%
60.8%
13.0%
52.4%
22.9%
51.0%
11.3%
53.3%
2.37%
2.96%
44.9%
1.09%
2.34%
0.99%
7.94%
0.88%
6.97%
1.90%
57.4%
37.3%
52.9%
1.13%
74.9%
21.8%
80.2%
10.9%
73.6%
17.5%
% KI-67+
C
CD45.2 Vascular
CD103
6.30%
0%
96.5%
1.17%
90.0%
3.70%
2.13%
0.15%
% CD45.2+ (Vascular)
D
CD127
KLRG1
65.6%
6.40%
5.75%
1.57%
63.1%
10.8%
52.8%
1.54%
84.8%
2.12%
17.6%
10.4%
44.5%
48.2%
14.1%
11.9%
36.0%
9.64%
11.3%
1.75%
% CD127+ KLRG1-
% KLRG1+ CD127-
% CD127+ KLRG1-
% KLRG1+ CD127-

Fig. 2

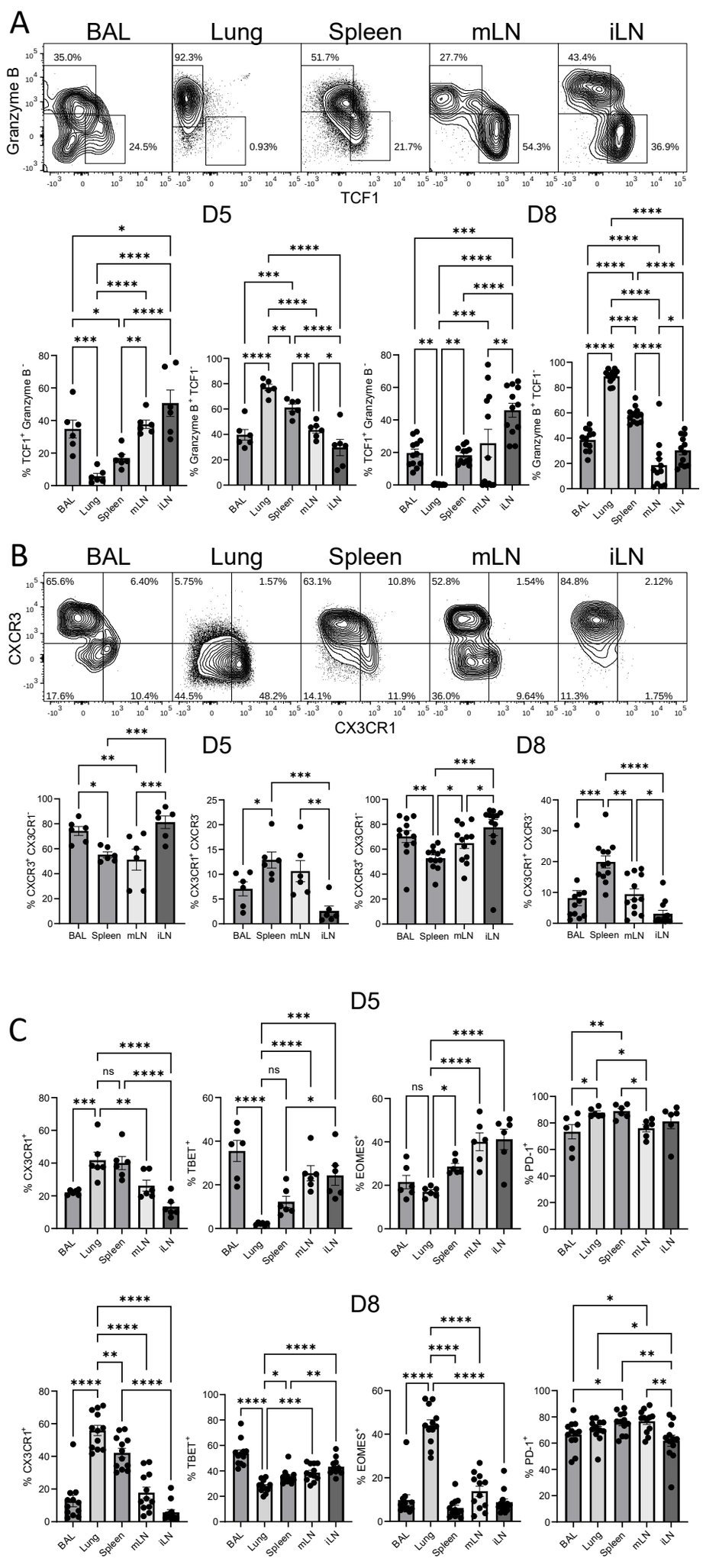
A
BAL
Lung
Spleen
mLN
iLN
Granzyme B
TCF1
35.0%
24.5%
92.3%
0.93%
51.7%
21.7%
27.7%
54.3%
43.4%
36.9%
D5
D8
% TCF1+ Granzyme B-
% Granzyme B+ TCF1+
% TCF1+ Granzyme B-
% Granzyme B+ TCF1+
B
CXCR3
CX3CR1
65.6%
6.40%
17.6%
10.4%
5.75%
1.57%
44.5%
48.2%
63.1%
10.8%
14.1%
11.9%
52.8%
1.54%
36.0%
9.64%
84.8%
2.12%
11.3%
1.75%
% CXCR3+ CX3CR1-
% CX3CR1+ CXCR3
% CXCR3+ CX3CR1-
% CX3CR1+ CXCR3-
C
D5
D8
% CX3CR1+
% TBET+
% EOMES+
% PD-1+

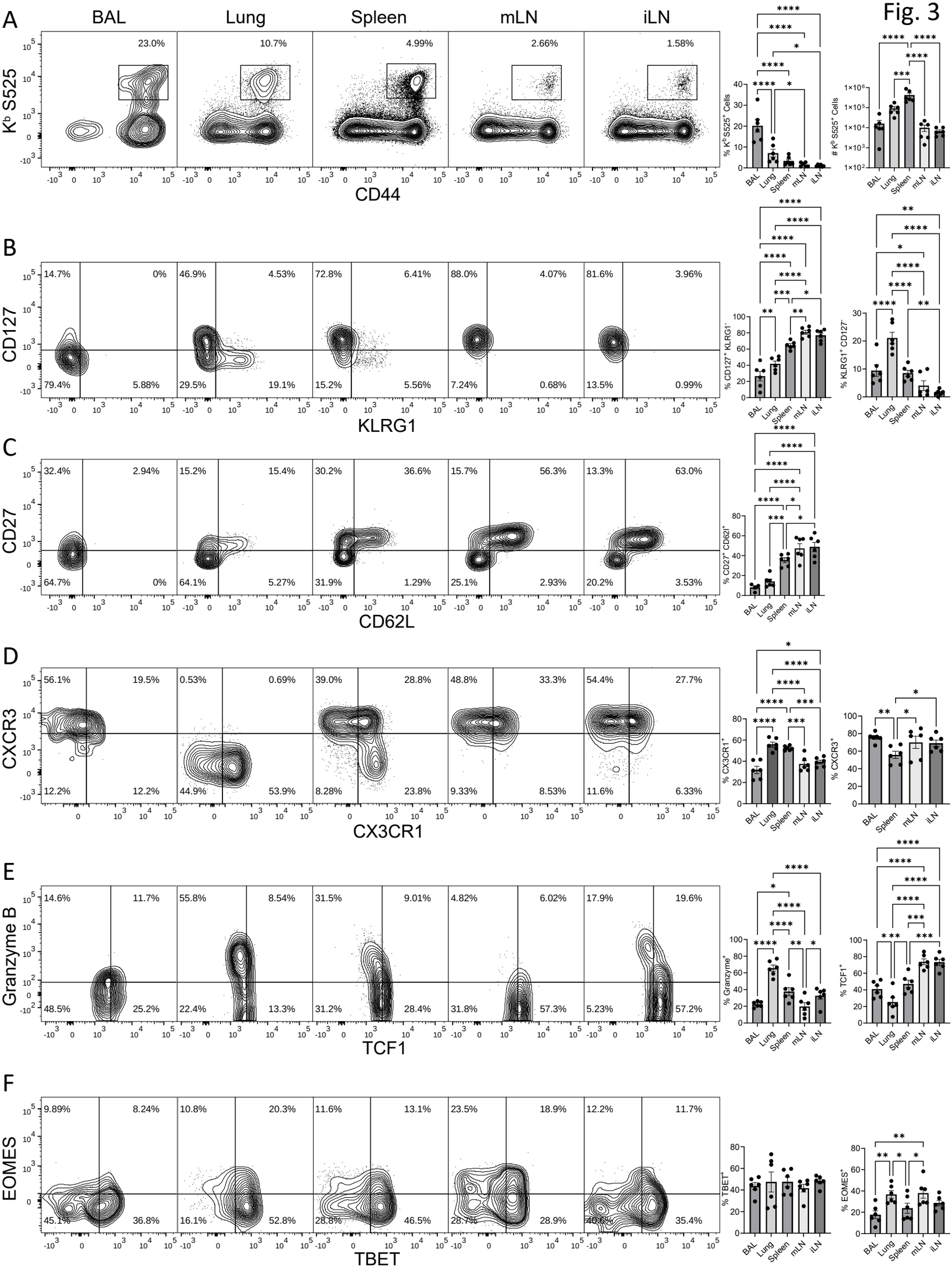
A
BAL
Lung
Spleen
mLN
iLN
23.0%
10.7%
4.99%
2.66%
1.58%
Kb S525
CD44
% Kb S525+ Cells
# Kb S525+ Cells
B
14.7%
0%
46.9%
4.53%
72.8%
6.41%
88.0%
4.07%
81.6%
3.96%
79.4%
5.88%
29.5%
19.1%
15.2%
5.56%
7.24%
0.68%
13.5%
0.99%
CD127
KLRG1
% CD127+ KLRG1-
% KLRG1+ CD127-
C
32.4%
2.94%
15.2%
15.4%
30.2%
36.6%
15.7%
56.3%
13.3%
63.0%
64.7%
0%
64.1%
5.27%
31.9%
1.29%
25.1%
2.93%
20.2%
3.53%
CD27
CD62L
% CD27+ CD62L+
D
56.1%
19.5%
0.53%
0.69%
39.0%
28.8%
48.8%
33.3%
54.4%
27.7%
12.2%
12.2%
44.9%
53.9%
8.28%
23.8%
9.33%
8.53%
11.6%
6.33%
CXCR3
CX3CR1
% CX3CR1+
% CXCR3+
E
14.6%
11.7%
55.8%
8.54%
31.5%
9.01%
4.82%
6.02%
17.9%
19.6%
48.5%
25.2%
22.4%
13.3%
31.2%
28.4%
31.8%
57.3%
5.23%
57.2%
Granzyme B
TCF1
% Granzyme+
% TCF1+
F
9.89%
8.24%
10.8%
20.3%
11.6%
13.1%
23.5%
18.9%
12.2%
11.7%
45.1%
36.8%
16.1%
52.8%
28.8%
46.5%
28.7%
28.9%
40.8%
35.4%
EOMES
TBET
% TBET+
% EOMES+
BAL
Lung
Spleen
mLN
iLN

Fig. 4

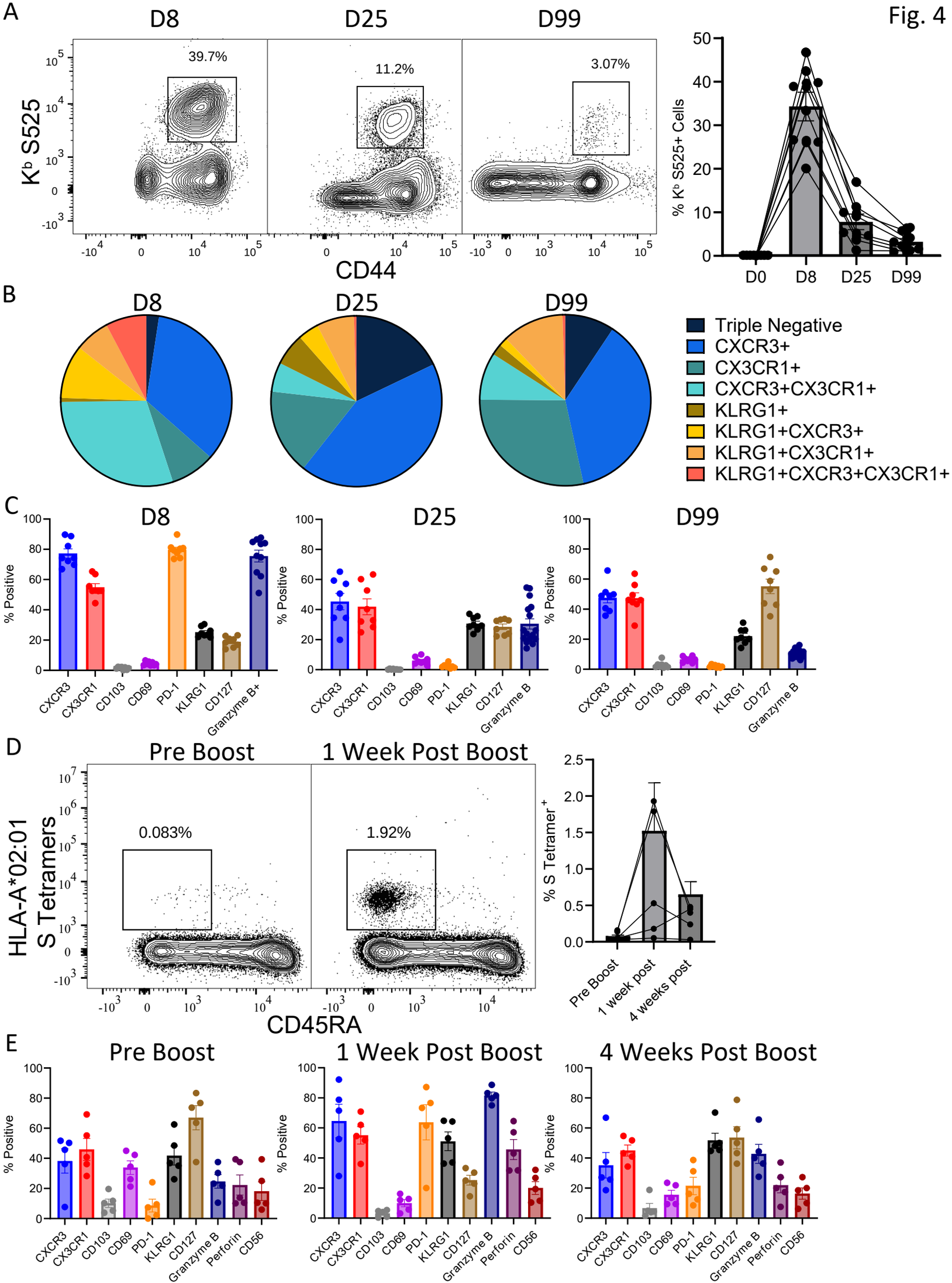
A
D8
D25
D99
39.7%
11.2%
3.07%
Kᵇ S525
CD44
% Kᵇ S525+ Cells
D0
D8
D25
D99
B
D8
D25
D99
Triple Negative
CXCR3+
CX3CR1+
CXCR3+CX3CR1+
KLRG1+
KLRG1+CXCR3+
KLRG1+CX3CR1+
KLRG1+CXCR3+CX3CR1+
C
D8
D25
D99
% Positive
CXCR3
CX3CR1
CD103
CD69
PD-1
KLRG1
CD127
Granzyme B+
Granzyme B
D
Pre Boost
1 Week Post Boost
0.083%
1.92%
HLA-A*02:01 S Tetramers
CD45RA
% S Tetramer⁺
Pre Boost
1 week post
4 weeks post
E
Pre Boost
1 Week Post Boost
4 Weeks Post Boost
% Positive
CXCR3
CX3CR1
CD103
CD69
PD-1
KLRG1
CD127
Granzyme B
Perforin
CD56

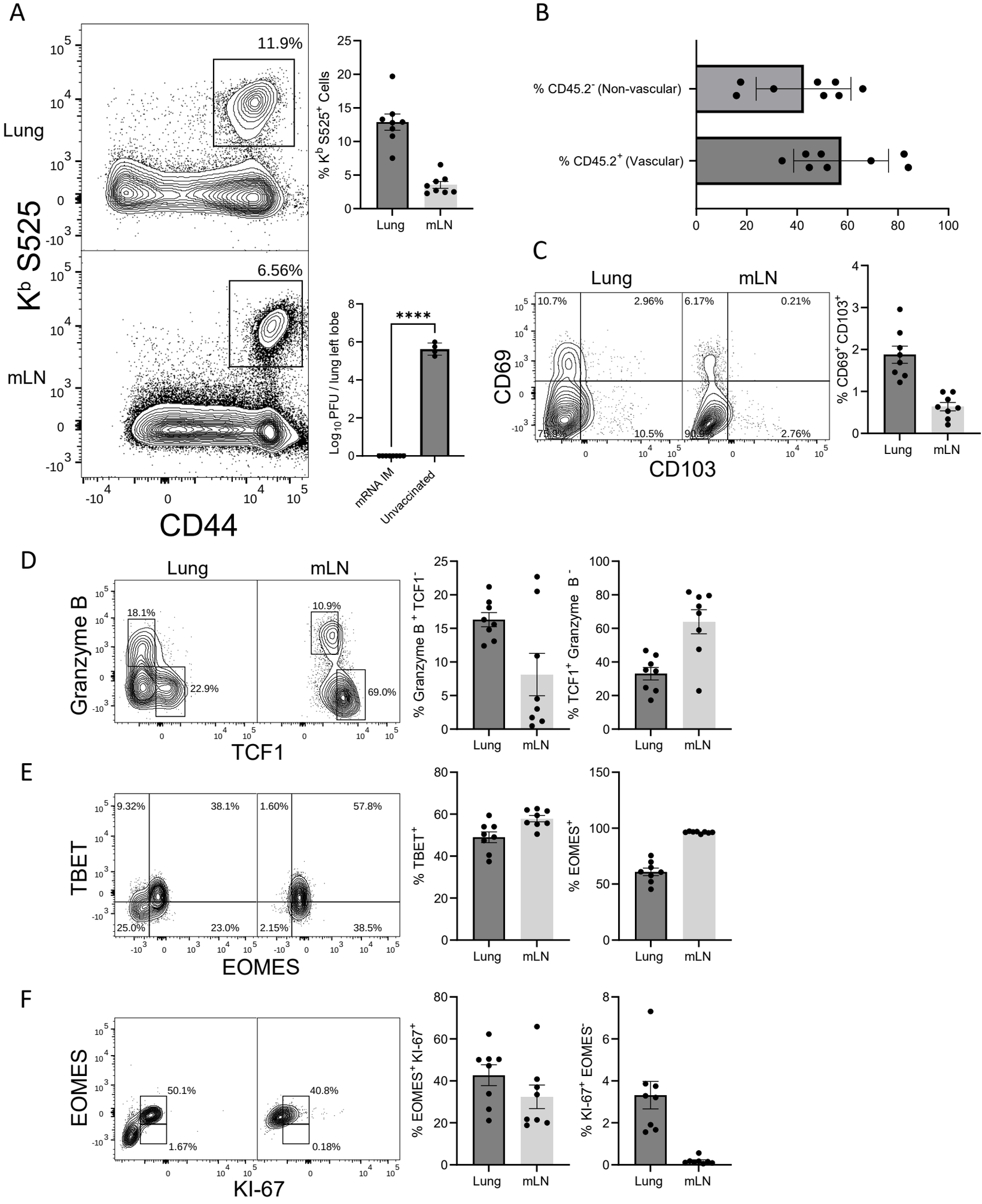
A
Lung
mLN
11.9%
6.56%
Kb S525
CD44
% Kb S525+ Cells
Lung
mLN
Log10 PFU / lung left lobe
****
mRNA IM
Unvaccinated
B
% CD45.2- (Non-vascular)
% CD45.2+ (Vascular)
C
Lung
mLN
10.7%
2.96%
6.17%
0.21%
10.5%
2.76%
CD69
CD103
% CD69+ CD103+
D
Granzyme B
TCF1
18.1%
22.9%
10.9%
69.0%
% Granzyme B + TCF1-
% TCF1+ Granzyme B -
E
TBET
EOMES
9.32%
38.1%
1.60%
57.8%
25.0%
23.0%
2.15%
38.5%
% TBET+
% EOMES+
F
EOMES
KI-67
50.1%
1.67%
40.8%
0.18%
% EOMES+ KI-67+
% KI-67+ EOMES-

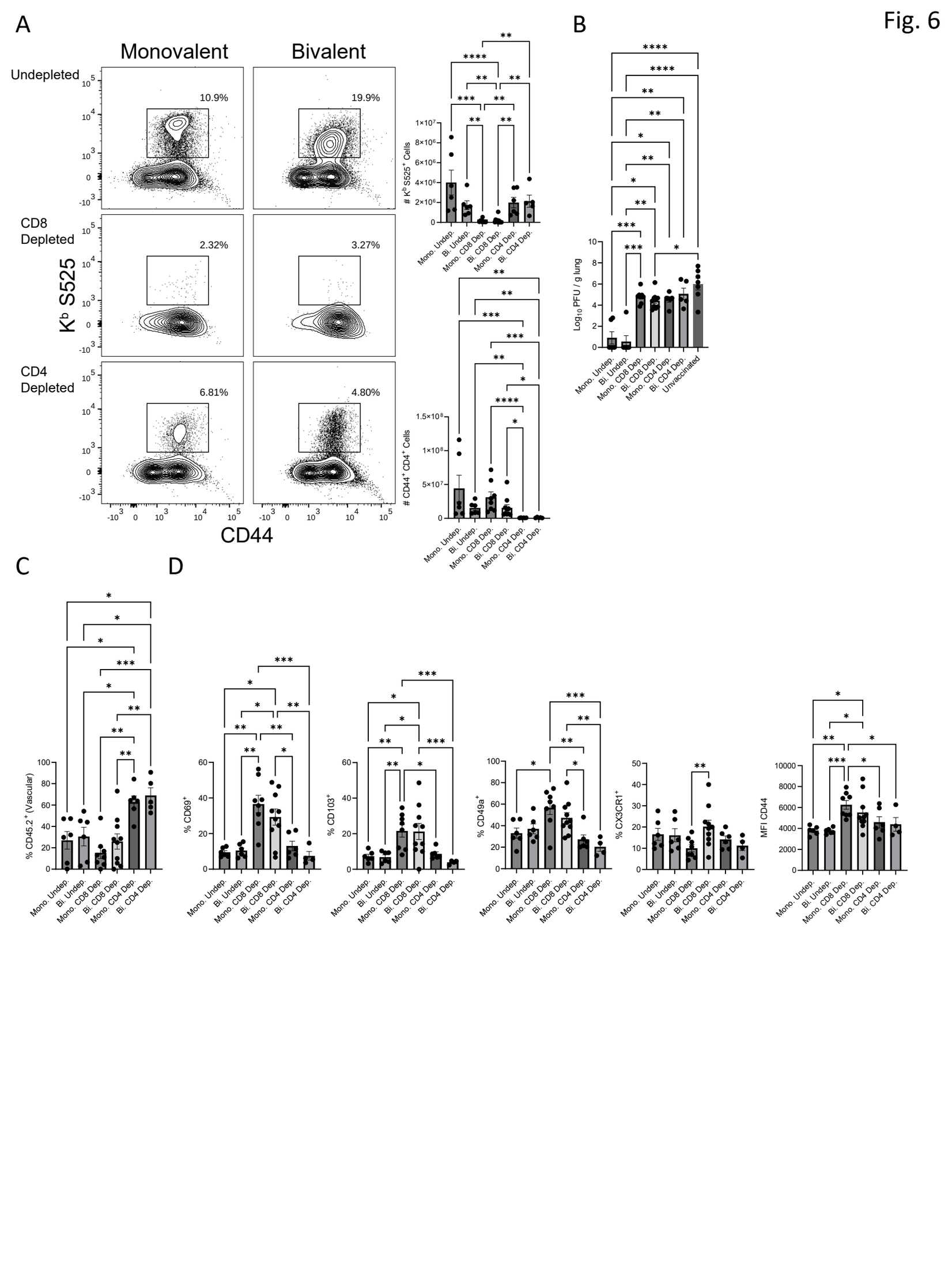
A
Monovalent
Bivalent
Undepleted
CD8 Depleted
CD4 Depleted
10.9%
19.9%
2.32%
3.27%
6.81%
4.80%
Kb S525
CD44
Kb S525+ Cells
CD44+ CD4+ Cells
B
Log10 PFU / g lung
Mono. Undep.
Bi. Undep.
Mono. CD8 Dep.
Bi. CD8 Dep.
Mono. CD4 Dep.
Bi. CD4 Dep.
Unvaccinated
C
% CD45.2+ (Vascular)
D
% CD69+
% CD103+
% CD49a+
% CX3CR1+
MFI CD44

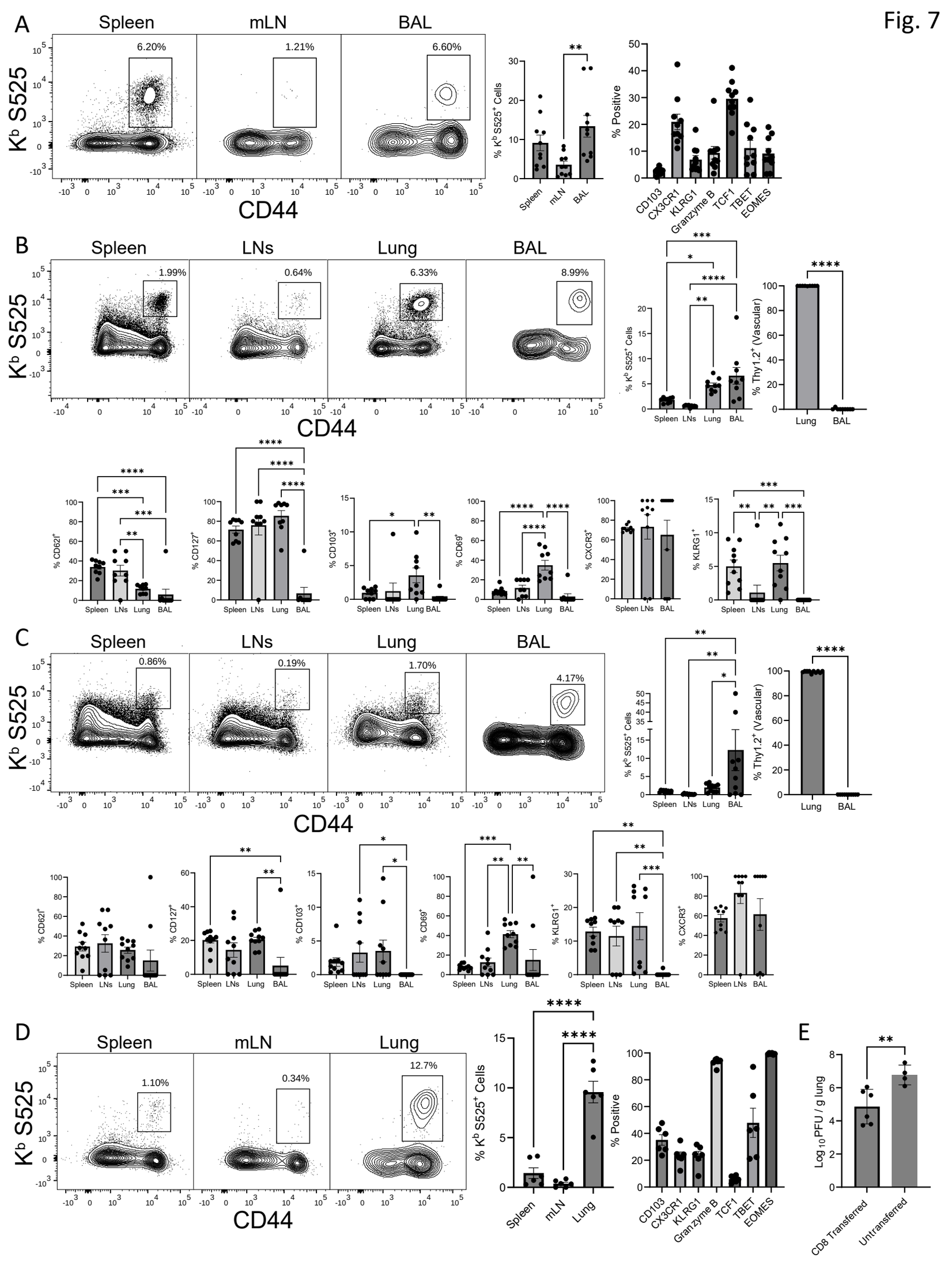
A
Spleen
mLN
BAL
6.20%
1.21%
6.60%
Kb S525
CD44
% Kb S525+ Cells
% Positive
CD103
CX3CR1
KLRG1
Granzyme B
TCF1
TBET
EOMES
B
Spleen
LNs
Lung
BAL
1.99%
0.64%
6.33%
8.99%
% Thy1.2+ (Vascular)
% CD62L+
% CD127+
% CD103+
% CD69+
% CXCR3+
% KLRG1+
C
0.86%
0.19%
1.70%
4.17%
D
1.10%
0.34%
12.7%
E
Log10 PFU / g lung
CD8 Transferred
Untransferred